Stope deformation measurements as a diagnostic measure of rock behaviour: a decade of research

by D.F. Malan*, J.A.L. Napier†, and A.L. Janse van Rensburg*

Transaction Paper

Synopsis

This paper presents an overview of work conducted over several years to investigate the continuous stope closure profiles recorded in tabular excavations and the use of this data as a hazard indicator. In spite of the brittle nature of the rock, measurements in gold mines and intermediate depth platinum mines revealed a significant time-dependent closure component. Various approaches to simulate the time-dependent closure have been investigated. Viscoelastic theory is able to simulate the time-dependent closure behaviour, but there are subtle problems with the use of this theory as it cannot simulate the failure processes in the rock. To overcome these problems, continuum and discontinuum elasto-viscoplastic models were developed by the authors. Discontinuum models have the advantage of being able to simulate the creep behaviour of prominent discontinuities. Development of these models has led to useful insights into rock mass deformation and has made the numerical simulation of parameters, such as rate of mining, possible for the first time. A number of practical applications for the mining industry have been developed from this study. Among these are the delineation of geotechnical areas using closure data, use of the data as a hazard indicator and to give warning of large collapses in the platinum mines, identification of areas to be preconditioned in the gold mines, measurement of the effectiveness of preconditioning and improved data for support design, which includes the effect of mining rate.

Introduction

In 1995, an article appeared in this journal describing 'A viscoleastic approach to the modelling of the transient closure behaviour of tabular excavations after blasting' (Malan[1]). This was essentially the first step of many to gain an improved understanding of the time-dependent deformation observed in deep tabular stopes. This current paper sets out to review the study of continuous stope closure in South African hard rock mines conducted by the authors over the last decade. The study is a useful example of the preferred stepwise research and development path, namely:

- observation and measurement of a poorly understood phenomenon
- attempts to gain a quantitative description of the phenomenon using analytical and numerical experimentation
- application of the improved knowledge to develop practical tools to assist industry
- knowledge transfer to the industry and implementation of the new-generation tools to improve layout and support designs and to assist with hazard assessment and decision-making processes.

As will be shown later in this study, some significant practical applications were derived from this study. These applications were made possible by the significant research efforts during the early parts of this study.

Unfortunately 'fundamental' rock engineering research appears to have become unfashionable in recent years, resulting in numerous failed attempts to develop practical tools without the necessary groundwork of Steps 1 and 2. Although the lead-time may be long in cases involving fundamental research, significant breakthroughs can probably be achieved only by proper in-depth studies of poorly understood phenomena. It can be argued that the luxury of long lead times cannot be afforded in view of the 2003 Health and Safety Summit decision in which the mining-industry committed to 'zero fatalities, injuries and ill health by 2013'. In spite of this bold statement, it is nevertheless guaranteed that new challenges will be faced by the industry in the foreseeable future and there is scope to reopen the debate about the need for further basic research in rock engineering.

With regard to the closure behaviour of tabular stopes, the initial fundamental studies were undertaken in the SIMRAC projects GAP029 (Napier *et al.*[2]), GAP332 (Napier *et al.*[3]) and GAP601b (Napier *et al.*[4]). The efforts

* *Groundwork Consulting (Pty) Ltd, Johannesburg.*

† *School of Computational and Applied Mathematics, University of the Witwatersrand, Johannesburg.*

 SA ISSN 0038–223X/3.00 + 0.00. Paper received Jun. 2007; revised paper received Oct. 2007.

of these initial projects focused mainly on the gold mining sector and investigated various aspects of fracture zone behaviour. As the practical use of continuous closure measurements became evident, two further projects focused on the development of practical systems for the mining in industry, namely GAP705, Malan *et al.*[5] and GAP852, Malan *et al.*[6]. In 2004, the study was extended to carry out investigations in the platinum industry (Roberts *et al.*[7]; Malan *et al.*[8]) and this work continued with a further SIMRAC project in the 2006/2007 financial year (SIM 060202).

Figure 1 illustrates a typical continuous closure curve measured in a deep (≈ 1 400 m) Merensky Reef stope. Similar curves were obtained during the initial investigations in the gold mines. The obvious problem faced by the research team during the initial data collection phase was the prominent time-dependent nature of the closure behaviour. In the absence of any mining activity or change in geometry, the increase in closure appeared to persist for many days. This behaviour seemed remarkable considering the fact that these excavations are developed in hard brittle rocks, which were never considered to be prone to 'creep'. What made an in-depth study of this phenomenon critical was the wide acceptance of elastic theory since the early breakthroughs of rock engineering pioneers in the 1960s (Ryder and Officer[9], Salamon[10], Cook *et al.*[11]) and the number of elastic tabular solvers developed as a consequence (e.g. Napier and Stephanson[12]). Although elastic theory can simulate the far-field rock mass behaviour very well, it can clearly not simulate the time-dependent rock response seen in Figure 1. The consequences of the prominent time-dependent behaviour can be appreciated by examining the well-known concept of energy release rate (ERR)[13]. In numerical modelling programs, a convenient method to calculate ERR is given by the following formula (Ryder and Jager[13]):

$$ERR = \frac{1}{2}\sigma^{p} S^{P} \qquad [1]$$

where S^P is the convergence at the face prior to an additional mining step and σ^P is the absolute normal stress acting over the increment to be mined next.

When one examines Figure 1, it is clear that S^P is a function of time and it would therefore appear as if ERR should also increase as a function of time. As a consequence, faces left standing would have a higher ERR than faces being mined regularly. (This argument is obviously not valid as ERR is an elastic concept and the behaviour recorded in Figure 1 is distinctly inelastic.) Previously, Salamon[14], highlighted some of the subtle difficulties associated with the interpretation of ERR and indicated that the problem lies in the fact that the rock mass is assumed to behave as a linear elastic material with infinite strength. In these circumstances, it can be demonstrated that the energy balance associated with the mining of small increments of elastic material is such that the work done by the applied loading forces is equal to the sum of the strain energy in the mined volume of material and the strain energy change in the surrounding rock mass. This implies that there is no obvious connection between the released energy as computed using Equation [1] and potential seismic motions when an analysis is based on the assumption of a perfect elastic material. A major hurdle to improve the concept of elastic ERR is an improved understanding of the inelastic failure processes and the energy changes associated with this (see e.g. Napier[15]). As the inelastic processes clearly occur in a time-dependent fashion (Figure 1), the time component can obviously not be ignored.

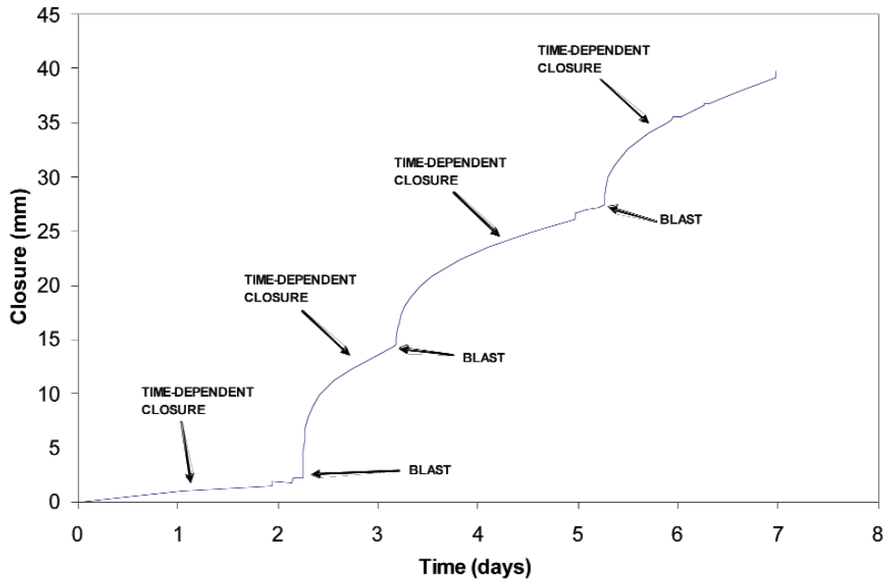

Figure 1—Typical continuous closure behaviour in a deep Merensky Reef stope

Definitions

In spite of the original terminology proposed by the ISRM[16] in 1975, the terms closure and convergence are often used interchangeably in the South African mining industry. An unofficial convention gradually adopted by many is that 'closure' refers to the relative movement of the hangingwall and footwall normal to the plane of the excavation as it is measured underground, whereas 'convergence' refers to the elastic component of closure. As this convention was firmly entrenched in the mid '90s in South Africa, this has been adopted by the authors. Furthermore, it became evident that it is necessary to distinguish between continuous and long-period closure measurements as defined below:

Long period closure measurements

These are discrete closure measurements with a typical interval of 24 hours or longer between successive observations of closure. These measurements are commonly plotted as a function of distance to face or time (usually in days or months). Figures 2 and 3 illustrate some examples. Note that if closure is plotted as a function of distance to face, the graph does not go through the origin as the closure instruments are always installed some distance behind the stope face and the measurement reflects the incremental movement after the time of installation.

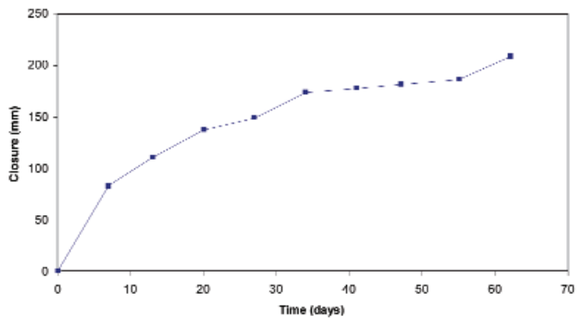

Figure 2—Typical closure curves obtained from long-period measurements. This data was recorded in a deep Merensky Reef stope

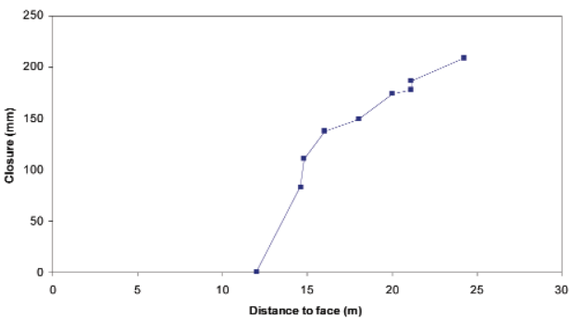

Figure 3—A typical closure curve obtained from long-period measurements where the closure is plotted as a function of distance to face. This data was recorded in a deep Merensky Reef stope

The data in Figures 2 and 3 was recorded by a closure station at a fixed location in a panel and, with time, the face moved away from the measurement point due to regular blasting. These results can therefore be misleading and very difficult to interpret as the curves are a complex aggregate of changes in face position and the time-dependent deformation of the rock.

Continuous closure measurements

In this case, closure is recorded continuously with suitable instrumentation such as clockwork closure meters. Closure collected with electronic data loggers with a sample frequency of greater than 1 sample/15 minutes will also be referred to as 'continuous'. These measurements are usually plotted as a function of time to illustrate the time component. An example is given in Figure 1. Note that the effects of changes in geometry and the time-dependent behaviour are clearly distinguishable since the sampling frequency is much greater than the intermittent face advance cycles.

Primary closure phase

This is the component of time-dependent closure following a blast and is characterized by a period (≈ 3 to 6 hours) of decelerating rate of closure. It is also observed after large seismic events in the gold mines.

Steady-state closure

This is the component of time-dependent closure following the primary closure phase (see Figure 4). The rate of steady-state closure appears to be constant in the short term but it gradually decreases when there is no blasting or seismic activity.

Instantaneous closure

The instantaneous closure component, ΔS_I, occurring during a seismic event or at blasting time (Figure 4). Owing to the delays in the detonation sequence between adjacent blast holes in the face, this closure phase is not really instantaneous at blasting time but can last for several minutes.

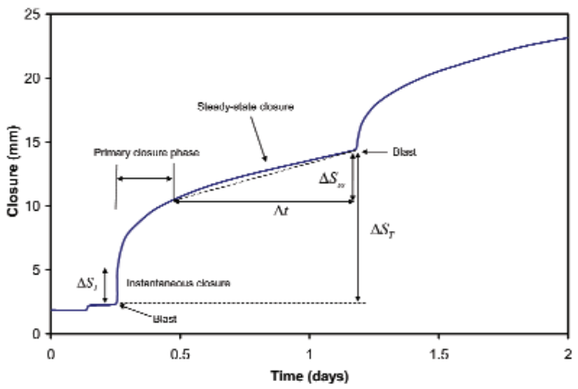

Figure 4—Typical continuous stope closure after blasting and the definition of closure terms

Rate of steady-state closure

Defined as

$$\dot{S}_{SS} = \frac{\Delta S_{SS}}{\Delta t} \qquad [2]$$

where ΔS_{SS} is the increase in steady-state closure over the time period Δt (see Figure 4). As the rate of steady-state closure gradually decreases in the absence of blasting activity, it is important to mention the period used for the calculation. The period Δt is often taken from six hours after the blast (to avoid the effect of the primary phase) to 24 hours after the blast (or until the next blast occurs, whichever comes first). The steady-state closure is therefore assumed to be linear function of time for the purposes of calculating Equation [2].

For elastic rock mass behaviour or inelastic behaviour that is not time dependent, it implies that $\dot{S}_{SS} = 0$ and

$$\Delta S_I = \Delta S_T \qquad [3]$$

Underground measurements in gold and platinum mines do not support the validity of Equation [3] even if the rock mass is very brittle (e.g. VCR stopes with a Ventersdorp lava hangingwall). It is found in almost all cases that $\Delta S_I < \Delta S_T$. The parameters ΔS_I, ΔS_{SS} and ΔS_T are found to be very useful to quantify different types of rock behaviour and motivate the value of carrying out continuous closure measurements. It is not possible to quantify these parameters when only long-term measurements are taken.

Historic overview of closure measurements

Some of the earliest references to stope closure in deep mines can be found in Altson[17] who referred to the closure as 'hangingwall subsidence'. It was noted that the rate of subsidence is a function of the area excavated, the elapsed time before the final support is installed and also the type and nature of support. Unfortunately no reference is made to the measurement technique or equipment or how the rate of subsidence was defined. The discussion in Altson's paper centred on how to limit the rate of subsidence as it was felt that this would decrease the incidence of rockbursting.

An interesting report on closure measurements (termed 'hangingwall sag') by R.K. Bradley was published as part of the discussion of a paper by Mickel[18]. Mickel suggested that waste packing results in a much delayed rate of subsidence. Bradley's report is the earliest known reference to continuous closure measurements. He was appointed as 'Investigator, Pressure Bursts and Hangingwall Sag' at the Eastern Section of Crown Mines, Ltd. and used a 'Tape-type Sagmeter' to record the closure. An example of the closure data is illustrated in Figure 5. The mechanism of his closure instrument (Figure 6) is essentially similar to the clockwork closure meters still recently used (Malan[19]). Bradley tried to relate the time-dependent closure to the deformation mode of the hangingwall beam and postulated that the closure profiles may possibly be used to predict rockbursts. It is, however, unclear if he did eventually achieve any success with this method.

Hill[20] described experiments conducted at ERPM where the average sag in two panels with different support types was compared. He suggested that the rate of sag depends on the intensity of pressure in the intact ground ahead of the face.

The term 'sag' was eventually replaced with 'closure' as can be seen in a paper by Barcza and Von Willich[21]. They conducted measurements of closure and ride at Harmony Gold Mine. The instrumentation consisted of a roofbolt in the hangingwall vertically above a horizontal plate in the footwall. Measurements were taken by suspending a plumb bob from the bolt and noting its length and position on the baseplate (similar to Wiggill's[22] technique illustrated in Figure 8). The horizontal and vertical movements were then converted to displacement normal and parallel to the reef plane to give closure and ride respectively. An attempt was also made to determine how much of the closure was from hangingwall sag and how much from footwall rise. By assuming a peg near the shaft as a datum, surveying techniques indicated that the closure consisted of 60% hangingwall sag and 40% footwall rise.

Leeman[23] used closure recorders developed by the CSIR and SMRE (Safety in Mines Research Establishment, England) to measure continuous closure profiles in a stope at East Rand Proprietary Mines (ERPM). These meters are essentially similar to those still in use (Malan[19]). He observed profiles similar to Bradley (in Mickel[18]) where the rate of closure suddenly increases just after blasting time (see Figure 7). This high rate of closure decreases within hours to give a gradual closure until the next blast occurs and the pattern repeats. On Sundays no blasting took place and, as expected, no incremental jump is visible in the data. The rate of gradual closure was usually also a minimum on Sundays. He concluded that the effect of blasting is to accelerate the gradual closure in a stope. Unfortunately, Leeman did not give any explanation for the observed closure profiles and he did not attempt to simulate this using either analytical or empirical approaches. He did note that the amount of closure caused by blasting diminishes with distance from the working face. The rate of closure also varied greatly from one point to the next and was affected by the position of the measuring point in relation to the support in the stope. He found no conclusive evidence that the rate of closure either

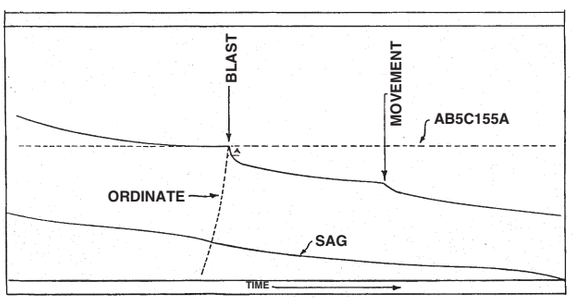

Figure 5—Continuous closure measurements recorded at Crown Mines (after Mickel[18]). Note that the closure increases downwards on the vertical axis

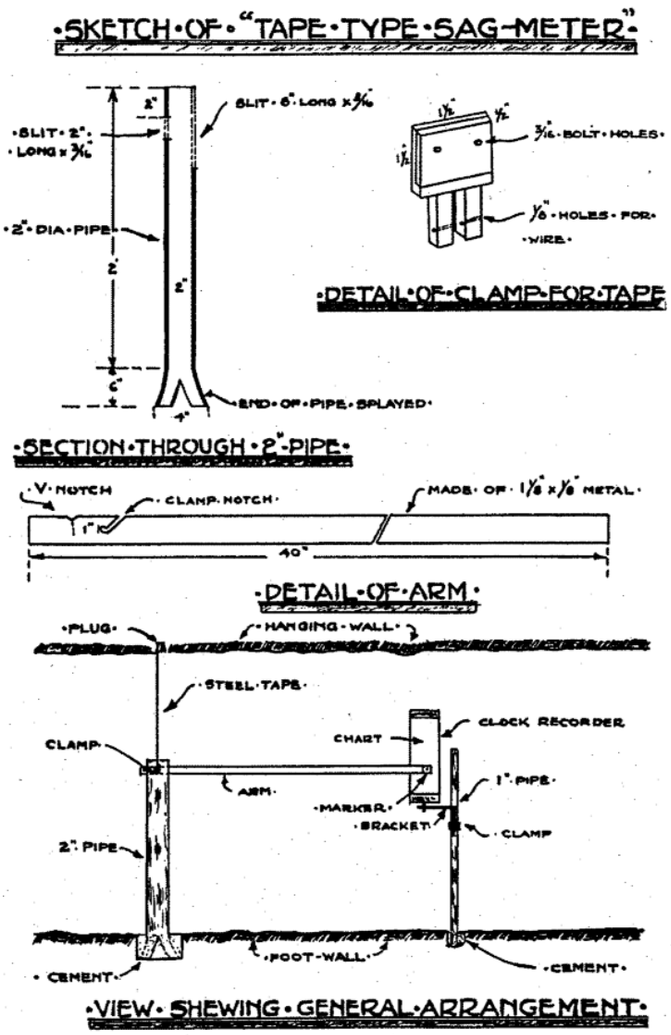

Figure 6—The 'tape-type sag meter' used by Bradley at Crown Mines (after Mickel[18])

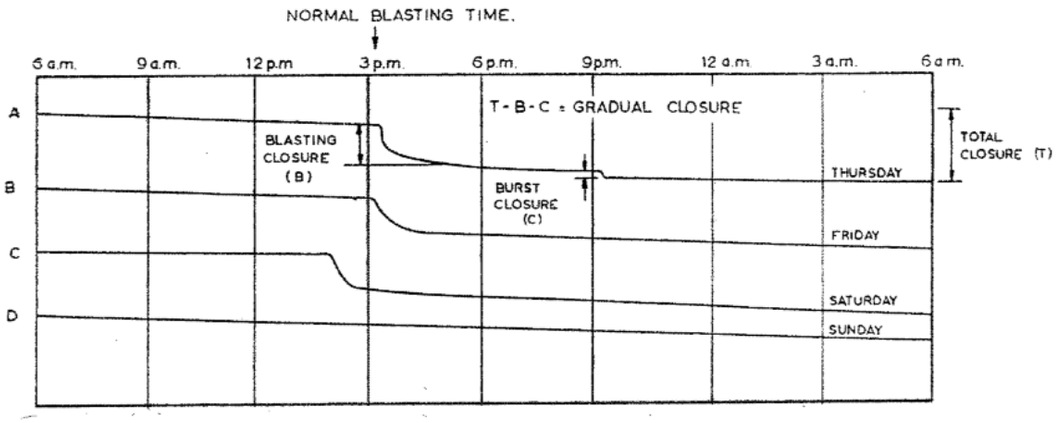

Figure 7—Typical continuous closure profiles measured at East Rand Proprietary Mines (after Leeman[23]). Note that the closure is increasing downwards on the vertical axis

increases or decreases just before a rockburst, but emphasized that further measurements were necessary to verify this.

Wiggill[22] measured closure and ride at Blyvooruitzicht and West Driefontein Mines to assess the effect of regional waste-pack stonewalls on the behaviour of stopes. In comparison to Leeman's work, he focused on long-term closure measurements. His closure and ride meters consisted of three different types as illustrated in Figure 8. Wiggill found that the rate of stope closure is largely independent of the type of support used and that time-dependent closure occurred even when there was no increase in the stope span. He also investigated the individual contributions of the hangingwall and footwall to the closure as indicated in Figure 9.

An important development in the 1960s was the increasing use of elasticity theory to solve mine design problems and to predict displacements of the rock mass. Predictions based upon this theory have been substantiated by underground measurements (Ryder and Officer[9], Ortlepp and Nicoll[24]). This development would influence the way stope closure measurements were being analysed for the next three decades.

Hodgson[25] measured continuous closure at ERPM. With the rise of elastic theory to prominence, he then also referred to his data as 'convergence' measurements. He nevertheless recognized that only the far-field rock behaviour is adequately described by elastic theory and the fracture zone around stopes is poorly understood. This probably motivated him to anchor his convergence meters a considerable distance into the hangingwall and footwall. The meters consisted of a nickel-chrome wire anchored in a borehole 16 m into the hangingwall. The wire extended through the stope to a cross-cut 16 m below the footwall where it was tensioned and attached to an LVDT (linear variable differential transformer). This allowed a continuous recording of the convergence on a magnetic tape. He found that over a long period of time, convergence measured by these anchored instruments corresponded to the elastic displacements resulting from changes in geometry. A more detailed examination of the manner in which the convergence takes place indicated that it is time dependent. He explained this by suggesting that there is a time dependent migration of the fracture zone ahead of the face resulting in the effective stope span becoming bigger. Hodgson predicted that, if the face advanced faster than the migration of the fracture zone, less energy would be released in a stable manner, thereby increasing the incidence of rockbursts.

The first quantitative attempt to analyse time-dependent closure was made by McGarr[26] using Hodgson's data from ERPM. He investigated the rate of convergence throughout

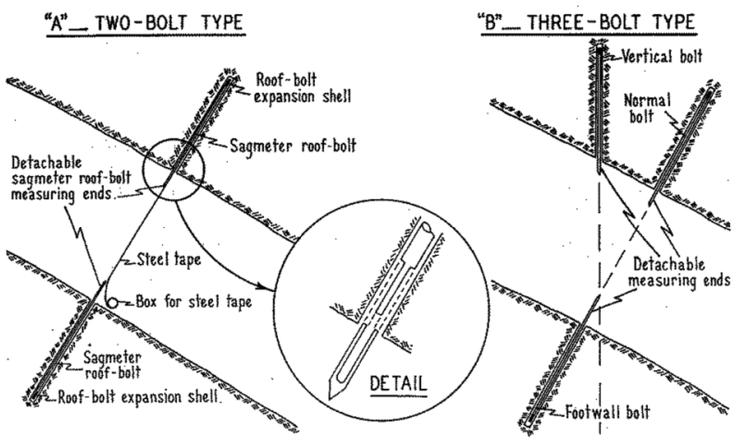

Fig. 2—Sketches of sagmeters

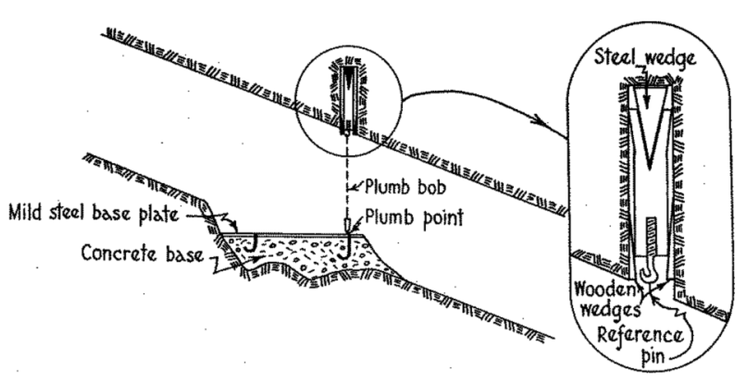

Figure 8—Closure and ride meters used by Wiggill at West Driefontein Mine (after Wiggill[22])

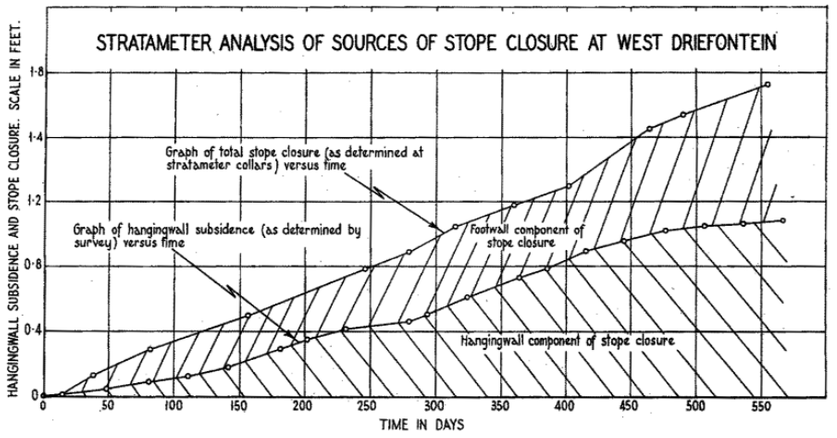

Figure 9—Contributions of hangingwall and footwall movements to stope closure (after Wiggill[22])

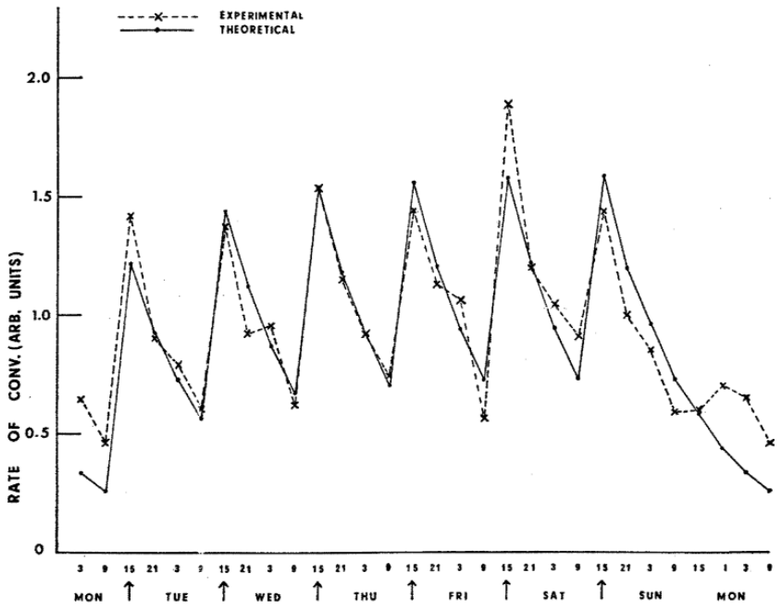

Figure 10—Stope convergence during six-hours intervals throughout the week at ERPM. The data have been averaged over 30 weeks. The time at the middle of each six-hour period is plotted on the graph (after McGarr 1971)

the week by using six-hourly intervals. The highest rate of closure was recorded during the six-hour interval, which included the blast. He found that the rate generally increases from Monday to Saturday, which suggested that during the week stress relaxation did not occur as fast as face advance (Figure 10).

McGarr[26] used an empirical approach to represent the closure δ as

$$\delta = \frac{B}{C} \sum_{n=0,n\neq 7m}^{\infty} \left(1 - e^{-DC(t-24n)}\right) H(t-24n) \qquad [4]$$

where *B, C* and *D* are positive constants, *n* and *m* are integers and *H* is the Heaviside unit function ($H(t) = 1$ for $t \geq 0$ and 0 for $t < 0$). The unit of time *t* in Equation [4] is hours. At the time of this study no blasting on Sundays was allowed and $n = 7m$ corresponds to those days. Obtaining the rate of closure from Equation [4] by differentiating gives

$$\dot{\delta} = DB \sum_{n=0,n\neq 7m}^{\infty} e^{-DC(t-24n)} H(t-24n) \qquad [5]$$

This equation is also plotted in Figure 10. After the last blasting period of the week on Saturday, the closure and the rate of closure become

$$\delta = a\left(1 - e^{-\frac{t}{\tau}}\right) \qquad [6]$$

and

$$\dot{\delta} = be^{-\frac{t}{\tau}} \qquad [7]$$

respectively where *a* and *b* are constants and $\tau = 1/DC$. McGarr[26] suggested that the relaxation time may be used as a parameter to describe the ability of the rock mass to form a

fracture zone in response to the face advance. High values of τ might be associated with mines that are prone to rockbursts.

For the next several years, the closure data collected in the industry was mainly long-period (low sampling frequency) measurements. Walsh *et al.*[27] measured convergence and ride at West Driefontein Mine with plum bob closure meters similar to those of Wiggill[22]. It was found that the convergence and ride are much greater than predicted by conventional elastic theory. In spite of the limitations of long-period measurements, some researchers noted significant time-dependent rock behaviour. King *et al.*[28] measured closure behaviour in two adjacent panels at Hartebeestfontein Mine. After blasting activity had stopped in one of the panels, the closure rate in this panel continued at a constant rate of 6 mm/day for 37 days. Only after this period did the rate gradually start to decrease. Mining continued in the second panel (and probably in other nearby panels) and it is unclear what the effect of these geometrical changes was on the first panel. After mining stopped in the second panel, the closure rate in this panel persisted for 13 days and then gradually declined.

Extensive closure data was collected by Gürtunca[29] to quantify the effect of backfill on stope behaviour. He noted that closure rates were significantly lower in filled stopes than in unfilled stopes (Gürtunca *et al.*[30], Gürtunca and Adams[31]). Many measurements of closure and ride were obtained with the 'four peg' method (Piper and Gürtunca[32]), which is illustrated in Figure 11. The change in the measured lengths between the footwall and hangingwall pegs is used to calculate the closure and ride components. Special instruments, which could be installed in the backfill, were also developed to allow for the remote monitoring of the closure (Piper *et al.*[33]). An electric closure meter is illustrated in Figure 12. The resistance of the potentiometer was remotely measured with an ohmmeter via the telephone cable. The measured resistance was proportional to the closure. These meters were not very reliable due to the extreme conditions in the backfill. Extensive use was therefore made of mechanical closure meters. This instrument consisted of two sliding tubes with a measuring wire attached to the inside of the one tube. This wire passes out through an angle junction into a closely wound spring of sufficient length to reach the gully. The measurement between the end of the wire that protrudes from the spring and the end of the spring is used to indicate the amount of closure. Comparison of measured closure in the backfill and elastic analyses indicated that the elastic convergence underestimates the real displacements (Gürtunca and Adams[31]). Gürtunca and Adams[32] suggested that a reduced elastic modulus be estimated from the closure data to be used in the elastic simulation programs.

Güler[34] did extensive long-period closure measurements of stopes in the Ventersdorp Contact Reef. Significant differences in closure rate were noted in different geotechnical areas. For areas with a soft lava hangingwall at East Driefontein Mine, a typical closure rate of 10 mm/day was measured, whereas it was 5 mm/day at Deelkraal Mine for the hard lava. It was unfortunately not clear what time periods he used to calculate these rates. He also noted that the closure rates are significantly affected by the mining rate.

Observations in different geotechnical areas

After 1994, renewed attention was paid to continuous stope closure measurements by the authors as part of the SIMRAC fracture zone research projects described in the introduction to this paper. Clear differences in the continuous closure

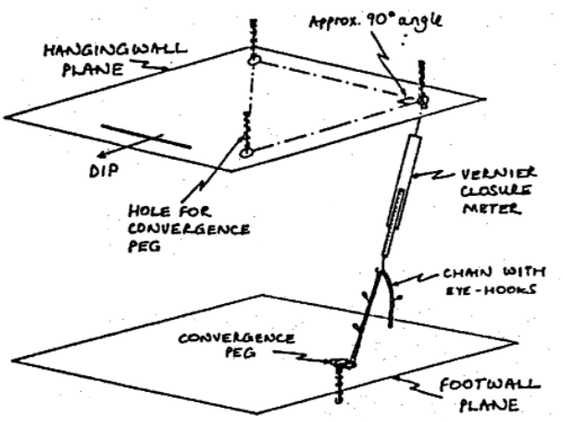

Figure 11—Illustration of the 'four peg' method to measure closure and ride (after Piper and Gürtunca[32])

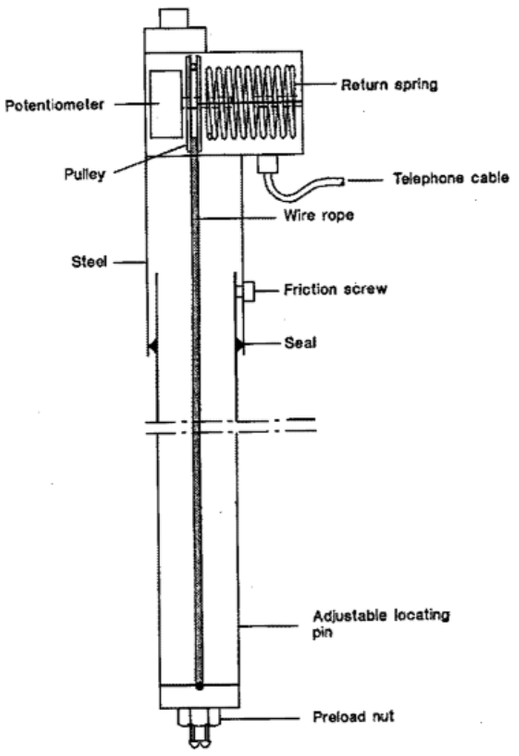

Figure 12—Electrical closure instruments used by Gürtunca to obtain long-period closure data inside backfill (after Piper *et al.*[33])

behaviour for different geotechnical areas were identified for the first time, which led to improved methods to assess rock mass behaviour in different mining areas. These observations are summarized in a number of papers (e.g. Malan and Napier[35], Malan[36] and Malan *et al.*[37]). For the gold mines, closure profiles with various $\Delta S_I/\Delta S_T$ ratios were observed. This provided valuable insight into the behaviour of the rock mass. Two extremes in behaviour are shown in Figure 13. Note that the $\Delta S_I/\Delta S_T$ ratios should be treated with some caution as the ΔS_I component is dependent on parameters such as distance to face (Malan[19]) and mining parameters (e.g. the length of face blasted on a particular day). It is currently not clear how useful the daily calculation of the $\Delta S_I/\Delta S_T$ ratio will be to improve short-term hazard assessments. It still requires further study and should be investigated only if the spatial positions of the closure meters and all other relevant parameters are meticulously recorded. Previous studies have nevertheless shown that an 'average' $\Delta S_I/\Delta S_T$ ratio observed over a period of time, appears to be very useful to distinguish between different geotechnical areas and to decide on appropriate mining strategies, such as the implementation of preconditioning.

It is of considerable interest that closure profiles very similar to that seen in the gold mines have been found in some of the stopes of the platinum industry at depth greater than 900 m. The observed closure profiles were found to be strongly dependent on geotechnical area. The characteristic profile shapes observed in each area proved to be very useful to obtain better insights into the rock mass behaviour. Two extreme closure profile examples are shown in Figure 14. In the majority of cases, it was found that the ΔS_{SS} component was lower than the two examples shown. Interesting profiles illustrating high rates of closure were also obtained in areas where the UG2 Reef was mined below Merensky remnants and where the middling between the reefs was small (< 20 m).

As expected, for the shallow platinum mines (< 400 m depth), the rates of closure are very low in the stable areas. An example is shown in Figure 15.

Development of appropriate models to simulate time-dependent rock behaviour

Numerical modelling of excavation behaviour has always been a powerful tool to gain insight into the mechanisms of rock deformation and to assist with layout and support design. Elastic theory still underpins most routine modelling exercises conducted in the industry. The prominent time-dependent rock behaviour seen in Figures 1, 13 and 14, however, indicates the need for an alternative approach to simulate the deformation of discontinuous rock masses.

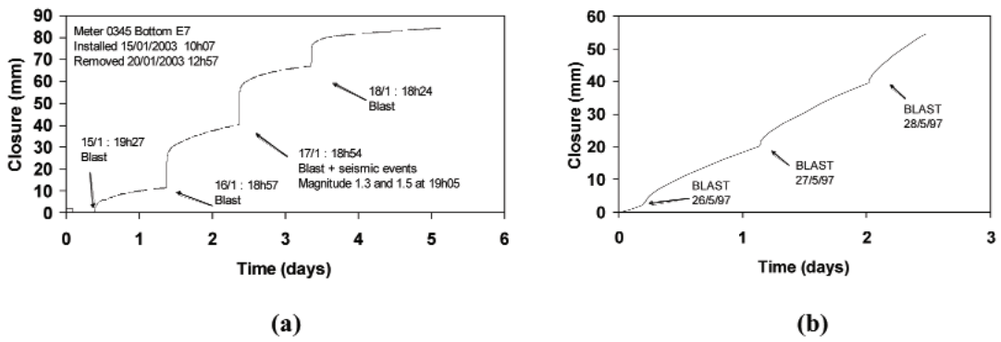

Figure 13—Continuous closure data collected from different geotechnical areas in the gold mines: (a) data from a VCR (Ventersdorp lava hangingwall) stope at Mponeng Mine with a high $\Delta S_I/\Delta S_T$ ratio and (b) data from a Vaal Reef stope at Hartebeestfontein Mine where ΔS_I is very small and $\Delta S_{SS} \approx \Delta S_T$. The differences in closure profiles from these two areas are very distinct

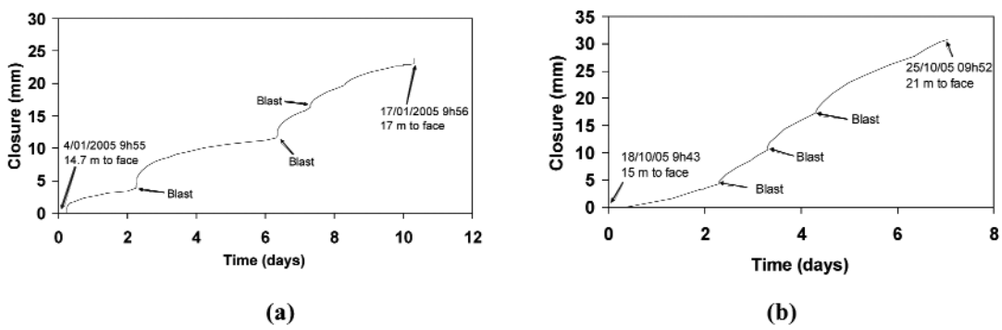

Figure 14—Continuous closure data collected from different geotechnical areas in the platinum mines: (a) data from a deep Merensky stope and (b) data from a deep UG2 stope

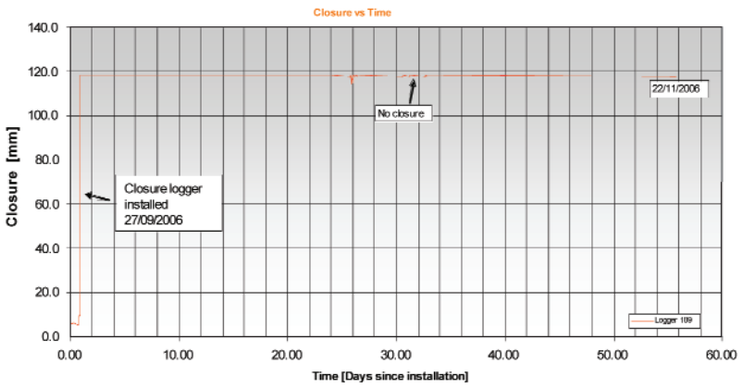

Figure 15—Closure recorded in a shallow UG2 panel

Use of viscoelastic theory

The theory of viscoelasticity provides a theoretical basis for analysing time-dependent rock movement and for extrapolation beyond the range of an experimental data set. In linear viscoelastic theory, complex strain-time behaviour can be described by various combinations of two principal states of deformation, namely elastic behaviour and viscous behaviour (Flügge[38]). The historical use of different viscoelastic models to simulate the creep of rocks is given in Lama and Vutukuri[39]. There has always been some doubt about the usefulness of this theory in representing rock behaviour (e.g. Robertson[40]), owing to the functional dependence of the viscosity values on stress, temperature and chemical environments. Similar to elastic theory, rock failure cannot be simulated. The use of viscoelastic material models have nevertheless found application in rock engineering and several publications can be found where viscoelasticity has been used to simulate time-dependent behaviour of rock (e.g. Pan and Dong[41]). In this current study, however, it was found that there are some subtle problems associated with the use of viscoelasticity theory to simulate time-dependent closure of tabular excavations in hard rock. These problems arise because of the special geometry of the tabular excavations and are not readily apparent when applying the theory to circular tunnels, as for example, in the study of Pan and Dong[41].

Viscoelastic convergence solution for tabular excavations

As a preliminary attempt to simulate the time-dependent deformations measured in tabular excavations, a viscoelastic approach was investigated. As no analytical model for the closure of tabular openings in viscoelastic media was available, a two-dimensional closure solution for a parallel-sided tabular excavation (Figure 16) in a viscoelastic medium was derived by Malan[1]. The original solution assumed a Kelvin viscoelastic model, but this was later improved by using a Burgers model (see Flügge[38] for a description of these different viscoelastic models). The solution was obtained by subjecting a known elastic solution to the viscoelastic correspondence principle (Malan[19]). An important feature of this analytical solution is that it accounts for the incremental enlargement of these excavations. When assuming that the rock behaves as an elastic material in dilatation and as a Burgers viscoelastic material (Figure 17) in distortion, the solution for an excavation developed in n increments with both faces blasted simultaneously can be derived as given in Equations [8] and [9]. The various coefficients in these two equations are given in Equations [10] to [19].

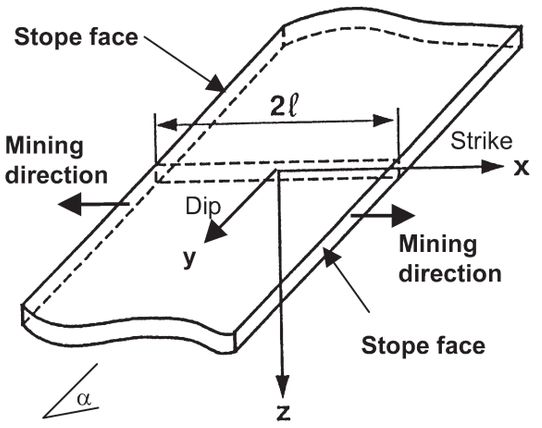

Figure 16—A single parallel-sided tabular excavation. The analytical viscoelastic convergence solution was derived for the two-dimensional section in the figure. The origin of the co-ordinate system is at the centre of the stope

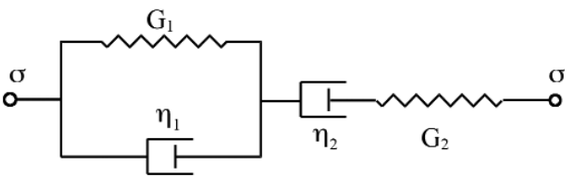

Figure 17—Representation of the Burgers viscoelastic model with the viscosity coefficients η_1 and η_2 and shear moduli G_1 and G_2

$$S_z = \left\{ \sum_{i=1}^{n-1} \left[S_z\left(\ell_i, t-\tau_i\right)\right] - \left[S_z\left(\ell_i, t-\tau_{i+1}\right)\right] \right\} + S_z\left[\ell_n, t-\tau_n\right] \quad \text{for} \quad \tau_n < t \le \tau_{n+1} \qquad [8]$$

where

$$S_z(\ell_i, t-\tau_i) = -4W_z\sqrt{\ell_i^2 - x^2}\,(1+\frac{dx}{2}) \times g_1\left[1 + c_5 t + c_6 e^{-f(t-\tau_i)} + \left\{c_7 \sinh b\left(t-\tau_i\right) + c_8 \cosh b\left(t-\tau_i\right)\right\} e^{\frac{-h(t-\tau_i)}{2}}\right] \qquad [9]$$

and

$$W_z = \frac{-\rho g H}{2}\left[(1+k)+(1-k)\cos 2\alpha\right] \qquad [10]$$

$$d = \frac{\sin\alpha\cos\beta}{H} \qquad [11]$$

$$b = \sqrt{\frac{\left(6Kp_1+q_1\right)^2 - 24K\left(6Kp_2+q_2\right)}{4\left(6Kp_2+q_2\right)^2}} \qquad [12]$$

$$g_1 = \frac{2Kp_1q_1 + q_1^2 - 2Kq_2}{4Kq_1^2} \qquad [13]$$

$$c_5 = \frac{2Kq_1}{2Kp_1q_1 + q_1^2 - 2Kq_2} \qquad [14]$$

$$c_6 = \frac{2K\left(p_2q_1^2 - p_1q_1q_2 + q_2^2\right)}{q_2\left(2Kp_1q_1 + q_1^2 - 2Kq_2\right)} \qquad [15]$$

$$c_7 = \frac{q_1^2\left(-12Kp_2q_1 + 6Kp_1q_2 - q_1q_2\right)}{2b\left(6Kp_2+q_2\right)^2\left(2Kp_1q_1 + q_1^2 - 2Kq_2\right)} \qquad [16]$$

$$c_8 = \frac{q_1^2q_2}{\left(6Kp_2+q_2\right)\left(-2Kp_1q_1 - q_1^2 + 2Kq_2\right)} \qquad [17]$$

$$f = \frac{q_1}{q_2} \qquad h = \frac{6Kp_1+q_1}{6Kp_2+q_2} \qquad [18]$$

$$p_1 = \frac{\eta_1G_2 + \eta_2G_1 + \eta_2G_2}{2G_1G_2}$$

$$p_2 = \frac{\eta_1\eta_2}{4G_1G_2} \qquad [19]$$

$$q_1 = \eta_2 \qquad q_2 = \frac{\eta_1\eta_2}{2G_1}$$

where S_z is the stope closure, $2\ell_i$ is the span of the stope after mining increment i, ρ is the density of the rock, x is the position in the stope relative to the centre, g is the gravitational acceleration, H is the depth below surface, k is the ratio of horizontal to vertical stress, α is the dip of the reef, β is the angle between the x-axis and the dip, υ is Poisson's ratio, E is Young's modulus, n is the number of increments, t is time and τ_i is the time when increment i is mined. The Burgers viscosity coefficients η_1 and η_2 and shear moduli G_1 and G_2 are defined in Figure 17. It should also be noted that this solution is valid only for stopes where a two-dimensional approximation is possible and where no contact between footwall and hangingwall occurs in the centre of the stope.

Using this approach, a good fit with experimental data could be obtained, as shown in Figure 18. Although this appears encouraging, problems were noted when attempting to calibrate the model at various distances from the mining face. These problems arise as the model predicts that the rate of steady-state convergence increases towards the centre of the stope. This can be shown by taking the time derivative of Equation [9] (assuming the excavation was made in a single cut, $i = 1$, at time $\tau_1 = 0$). For time $t \to \infty$, the derivative is given by (Malan[19])

$$\left.\frac{dS_z}{dt}\right|_{t\to\infty} = \frac{-2W_z\sqrt{\ell^2 - x^2}\left(1+\frac{dx}{2}\right)}{\eta_2} \qquad [20]$$

As $t \to \infty$, the rate of convergence rate in the steady-state phase is therefore only a function of geometric parameters, stress magnitude and the viscoelastic parameter η_2. This is intuitively expected from Figure 17. Also if $\eta_2 = \infty$ (thereby reducing the Burgers model to the 3-parameter solid, Equation (20) predicts correctly that at $t \to \infty$, the convergence rate becomes zero. The steady-state convergence rate (Equation 20) was plotted as a function of the position x in Figure 19. The highest rate of convergence is in the centre of the stope, which reduces to a value of zero at the stope face. This can be compared with some underground data collected in a South African mining stope (Figure 20), illustrating the opposite trend where the rate of steady-state closure decreases with increasing distance from the stope face. This difference in behaviour is caused by the inability of the viscoelastic model to simulate the fracture processes surrounding the deep mining excavations.

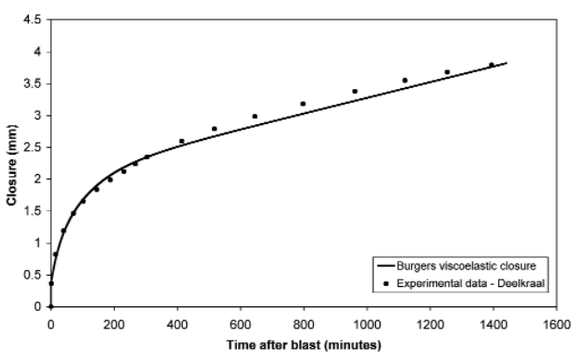

Figure 18—The Burgers viscoelastic closure solution fitted to experimental closure measured at Deelkraal Mine (after Malan[19])

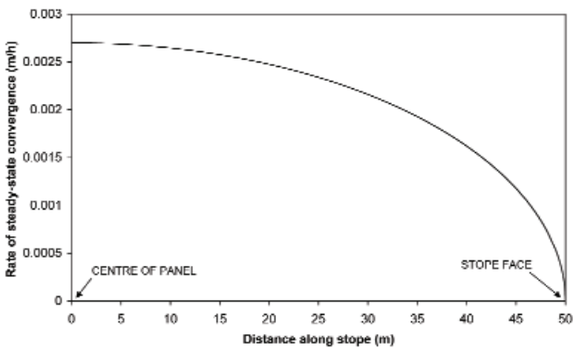

Figure 19—The rate of steady-state convergence along a panel of 100 m span at $t \rightarrow \infty$. Values used in this simulation are $\eta_2 = 2 \times 10^{12}$ Pa.h, H = 2000 m, $\alpha = 0°$, $k = 0.5$, $g = 9.81$ m/s^2 and $\rho = 2700$ kg/m^3

Figure 20—Closure data from a deep tabular mining stope in South Africa. Note that the rate of steady-state closure decreases as the distance to face increases. This is contrary to what is shown by the viscoelastic model in Figure 19 (note that the stope face is to the left in Figure 20 and to the right in Figure 19)

Continuum elasto-viscoplastic modelling

As concluded in the previous section, a viscoelastic approach is not entirely suitable to simulate the time-dependent behaviour of deep excavations in hard rock since time-dependent failure processes in the rock play a prominent role in the underground deformation behaviour. Any model used to simulate this time-dependent behaviour needs to include some representation of the delayed failure processes and the resulting time-dependent extension of the fracture zone. It appears as if the significant time-dependent effects are confined to the fracture envelope surrounding excavations. The far field behaviour has been shown to be adequately represented by elastic theory (Ryder and Officer[9]). To simulate this behaviour, it is therefore necessary that some constitutive model should be derived that is able to approximate the rheology of the fracture zone. To simulate the time-dependent fracture processes, a continuum elasto-viscoplastic model with a time-dependent cohesion weakening rule was developed and implemented in the finite difference computer code FLAC.

To include failure processes in rheological models, slider elements (also called St. Venant elements) are typically added to the elastic and viscous elements of viscoelasticity. These slider elements have a specified failure strength and are immobilized below this strength. Commonly, a dashpot is placed in parallel with the slider to control the strain rate if the slider is loaded above its failure strength. This is the so-called Bingham unit. Various combinations of elastic, viscous and St. Venant elements have been used by different researchers to simulate particular time-dependent problems. Gioda[42] and Gioda and Cividini[43] used a Kelvin unit in series with a Bingham unit to represent primary and secondary closure in squeezing tunnels. Tertiary movements can be considered by providing suitable laws relating the values of the mechanical parameters (such as viscosity) to the irreversible part of the time-dependent strain. These rheological models are particularly suited for analysis carried out through the finite element method. This allows the interaction between squeezing rock and support to be simulated. Other examples of the use of these rheological models can be found in Akagi *et al.*[44], Song[45] and Lee *et al.*[46].

Since Perzyna[47] proposed the general concept of elasto-viscoplasticity, a number of workers have applied this theory to geological materials. Elasto-viscoplasticity is essentially a modification of classical plasticity theory by the introduction of a time-rate rule in which the yield function and plastic potential function of classical plasticity are incorporated. In comparison with viscoelasticy, a viscoplastic material shows viscous behaviour in the plastic region only. Desai and Zhang[48] used this theory together with a generalized yield function to characterize the viscoplastic behaviour of a sand and rock salt. Sepehr and Stimpson[49] used Perzyna's theory as a basis to develop a time-dependent finite element model to understand the time-dependent closure of excavations and seismicity in the potash mines in Saskatchewan. Fakhimi and Fairhurst[50] proposed a visco-elastoplastic constitutive model to simulate the time-dependent behaviour of rock. The model consists of an elasto-plastic Mohr-Coulomb model in series with a linear viscous unit. This model was implemented in an explicit finite difference code. A typical solution cycle would be to perform an elasto-plastic analysis of failure at a given time. After an equilibrium point is reached, the linear viscous unit is used to determine additional creep strain components for a specified period of elapsed time. Control is then passed back to the elasto-plastic analysis to obtain a new equilibrium and the process is repeated. Although this model appeared successful in imitating the behaviour of uniaxial and triaxial tests and the stand-up time of excavations, the time-dependent behaviour of the model is independent of the failure processes. The entire material (including the far field) also behaves in a viscous manner. This model is therefore not applicable to the conceptual model of deep excavations in hard rock where the time-dependency is a direct consequence of the failure processes on discontinuity assemblies and the solid rock behaves essentially elastically.

A complete description of the model developed for this study can be found in Malan[51]. Figure 21 gives a representation of the developed model.

In this model, the intact rock behaves elastically, while a Mohr-Coulomb yield function determines the failure strength. Similar to classical viscoplasticity, the principal viscoplastic strain rate components, $\dot{\varepsilon}_i^{vp}$, after failure is given by

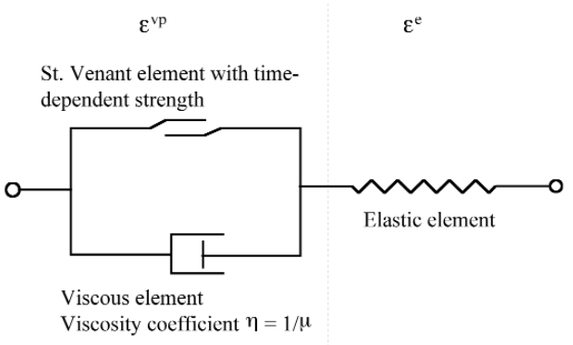

Figure 21—Representation of the developed elasto-viscoplastic model

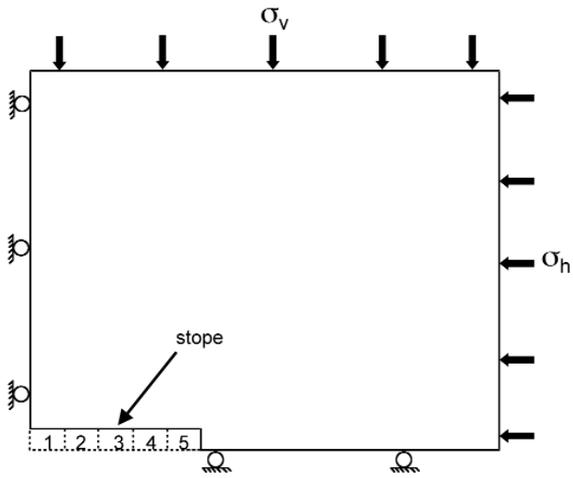

Figure 22—Geometry and boundary conditions used in FLAC to simulate the time-dependent behaviour of a tabular excavation

$$\dot{\varepsilon}_i^{vp} = \mu\left\langle f_s(t)\right\rangle \frac{\partial g_s}{\partial \sigma_i} \qquad \text{for} \quad i = 1, 2, 3 \qquad [21]$$

where μ is the fluidity parameter, g_s is the plastic potential function, $f_S(t)$ is the yield function and σ_i are the principal stress components. A constitutive description of time-dependent rock behaviour needs to include the effect of strength degradation with time and/or deformation. Observations of time-dependent fracturing ahead of tabular stopes and in some tunnels in the South African mines show that the rock becomes progressively more fractured with time, resulting in the gradual loss of cohesive strength in a particular volume of rock. This loss of strength was modelled by assuming that the rate of cohesion reduction C_c is proportional to the excess stress above the residual target surface.

$$\dot{C}_c = k_c\left\langle f_{res}\right\rangle \qquad [22]$$

where k_c is the cohesion decay factor and

$$f_{res} = \sigma_1 - \sigma_3 N_{\phi r} + 2C_r\sqrt{N_{\phi r}} \qquad [23]$$

$$N_{\phi r} = \frac{1+\sin\phi_r}{1-\sin\phi_r} \qquad [24]$$

is the residual target surface with C_r the residual cohesion and ϕ_r the residual friction angle. The principle embodied in Equation [22] is based on the laboratory creep experiments described in Malan[19] which indicated that if the rock specimens are loaded close to their failure strength, the creep rate and eventual creep failure occur faster than for a low stress. For a particular volume of rock under high stress, creep fractures will therefore form more rapidly, resulting in a faster loss of cohesion in the rock than for low stress.

To illustrate the behaviour of the model described above, Malan[52] simulated a tabular excavation to investigate the effect of mining rate. Figure 22 illustrates the geometry used in FLAC to simulate a tabular excavation.

A problem with this approach was that as the stope had to be mined in incremental fashion, very large computer run times were recorded. The explicit solution scheme of FLAC requires a small time-step to ensure stability. Following a large instantaneous stress change (for example, after a mining increment), the creep time-step must be very small. Only as a new equilibrium state is approached, can the time-step be progressively enlarged. This currently prohibits the simulation and calibration of incremental stope behaviour if the span is large.

The time-dependent nature of the constitutive model leads to the delayed development of the fracture zone around the stope (Figure 23). This enabled the model to simulate the closure behaviour seen underground (Figure 24). Calibration

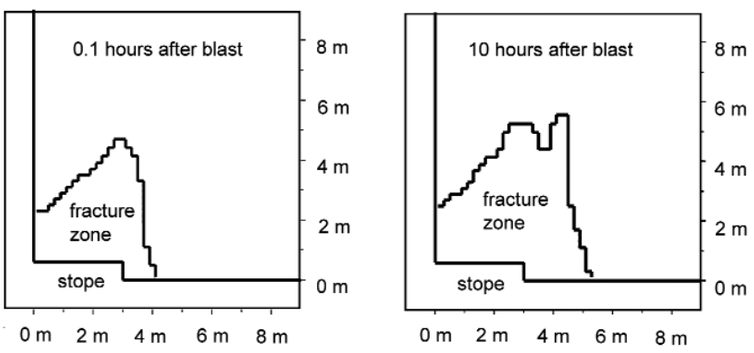

Figure 23—The simulated time-dependent extent of the fracture zone at (a) 0.1 hours after the mining increment and (b) 10 hours after the mining increment (after Malan[52])

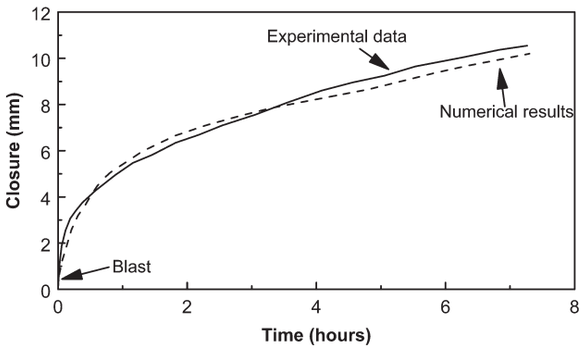

Figure 24—Experimental and simulated stope closure after blasting using a continuum elaso-visocplastic model (after Malan[52])

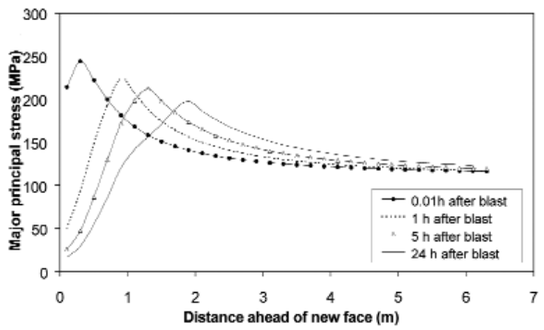

Figure 25—Time-dependent position of the stress peak ahead of a simulated stope in elasto-viscoplastic material after mining an increment

of the model from these closure measurements, however, proved to be problematic due to the large number of parameters present and the time-dependent nature of the constitutive model. The two-dimensional plane strain version of FLAC is used and therefore only geometries where these assumptions can be made are appropriate for calibration. As the results obtained from viscoplasticity theory are path dependent, the entire stope span cannot be simulated in one mining increment.

Following the success of the model to simulate the time-dependent nature of the fracture zone and the resulting closure, it was used to investigate rate of mining problems. As it is generally accepted that high stress peaks close to the face may increase the likelihood of face bursting (e.g. Nawrocki[53]), modelling was conducted to investigate how mining rate affects the position of the stress peak ahead of the face. As a result of the time-dependent nature of the simulated fracture zone, the stress peak ahead of the face is not stationary, but moves as a function of time. An example is given in Figure 25, which illustrates the simulated stress peak as a function of time. Soon after the blast the peak is high and located close to the face. With time it moves away, due to the fracture processes, gradually becoming smaller. Of significance is that the biggest stress change happens within the first five hours.

To investigate the effect of rate of mining, the stope in Figure 22 was mined at four different mining rates namely 1 m/2 hours, 1 m/12 hours, 1 m/24 hours and 1 m/48 hours. The stress peak after the fifth mining increment for each mining rate is given in Figure 26. The time used for plotting each peak corresponds to that time when the next increment is about to be mined.

Discontinuum elasto-viscoplastic model

An alternative approach to simulate time-dependent stope closure is to assume that the time-dependent behaviour of excavations is dominated by the creep of multiple individual discontinuities (Napier and Malan[54]). The discontinuity creep behaviour can be represented using interacting displacement discontinuity boundary elements in which the rate of slip, dD_y/dt, on a 'failed' discontinuity is assumed to be proportional to the driving shear stress τ_e. Specifically,

$$\frac{dD_y}{dt} = \kappa\tau_e \qquad [25]$$

where κ is designated as the surface fluidity having units of m/(Pa·s).

It was found that by modelling a stope surrounded by a random mesh of potential cracks and using the approach outlined above, time-dependent closure profiles similar to that observed underground can be simulated. An example is shown in Figure 27.

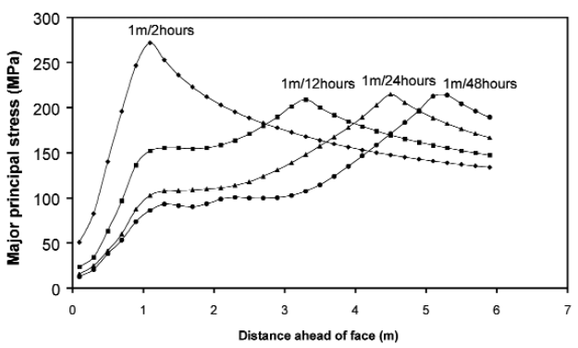

Figure 26—Effect of mining rate on the nature of the stress peak ahead of the stope face

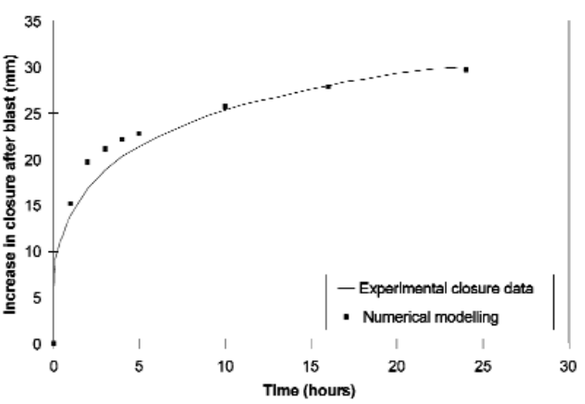

Figure 27—Simulating time-dependent stope closure using a viscoplastic discontinuum model (after Napier and Malan[54])

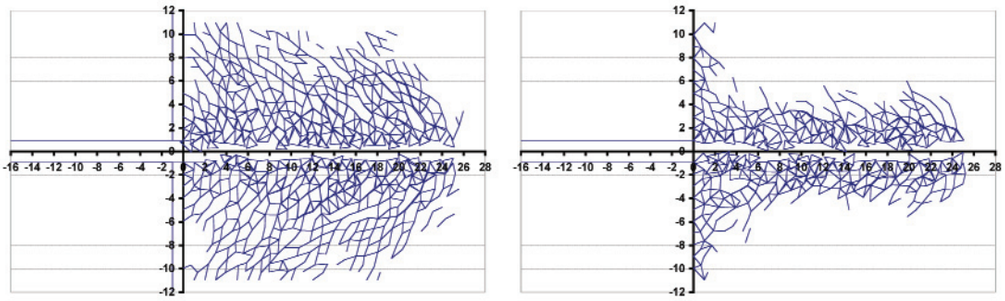

Figure 28—Distorted grid plots of fracture zone formation after twenty-five mining steps in (a) 'low' strength and (b) 'high' strength rock

A further example of using this approach is found in Malan *et al.*[55]. In this study, fracture zone development was modelled by extending one side of a parallel-sided, horizontal mining panel towards a region covered by a random mesh of potential cracks. The random mesh was generated using a Delaunay triangulation scheme. The failure properties of the mesh positions are determined by a Mohr-Coulomb criterion with specified cohesion and internal friction angle. Two cases were considered: a 'low' strength rock with cohesion equal to 15 MPa and a 'high' strength rock with cohesion equal to 25 MPa. In each case the internal friction angle was chosen to be 45 degrees. The mining simulation was carried out in 25 face advance steps of one metre starting from an initial span of 50 m. Following each mining step, twenty-four time relaxation steps were allowed to occur. Within each time relaxation step, the stress state is examined at each element of the random mesh and, if the stress exceeds the specified Mohr-Coulomb intact limit, these elements are allowed to slip at a rate determined by Equation [25]. The driving shear stress τ_e is computed to the difference between the shear stress and a specified residual frictional resistance that was set to 30 degrees. Closure 'measurements' were performed by computing the difference in vertical displacement arising between benchmark points located 2 m in the hangingwall and 2 m in the footwall at each of five monitoring positions. These closure 'stations' were spaced at intervals of 5 m with the measuring points of the first station aligned vertically above and below the centre of the first excavation increment.

Figure 28 show the fracture zone developed after 25 mining steps in the random mesh for the 'low' and 'high' strength rock environments. In these plots, the hangingwall region is separated from the footwall region to display the distorted deformations more clearly (including some detached fragments). It can be seen that a much larger region of rock is activated in the low strength material as would be expected intuitively. It is apparent also that considerable fragmentation of the rock occurs at the boundaries of the hangingwall and the footwall. Typical closure profiles observed for the low and high strength rock cases, are shown in Figure 29. These profiles show a marked difference in deformation behaviour between the two material models. It should be noted that the explicit discontinuity slip simulation can be extended to include features such as parting planes or pre-existing fault planes near the stope face.

Practical applications of continuous closure measurements

Apart from the benefits of using continuous closure to identify different geotechnical conditions and tailoring layout and support designs to cater for this, a number of other practical applications of these measurements became evident during the course of these studies. Some of these are listed below.

Identification of hazardous areas and warning of large panel collapses

In the platinum industry, use of closure measurements to identify hazardous conditions has found extensive application and a number of mines are currently taking these measurements on a routine basis. Apart from the normal electronic closure loggers, closure telltales with a traffic light system to warn of hangingwall movements have now also been developed and these are currently being implemented in the first mine. These developments have been based on studies that showed that in a number of cases, advance warning of several days have been obtained prior to large collapses. Two examples are illustrated below, namely collapses in Merensky and UG2 panels. A further example can be found in Malan *et al.*[37].

For the collapse in the Merensky panel, the layout and positions of the instrumentation at this site are given in Figure 30. Breast mining occurs on the Merensky Reef at approximately 1 400 m below surface. The intersection of

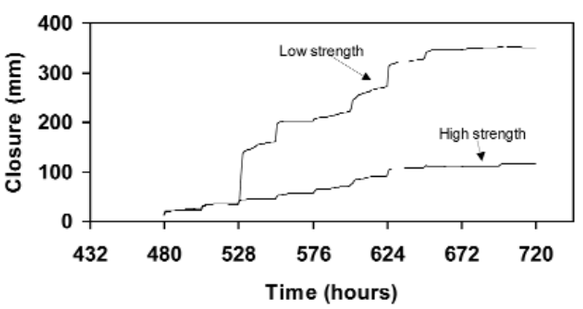

Figure 29—Typical closure profiles simulated for 'low' and 'high' strength rock materials using a viscoplastic discontinuum model

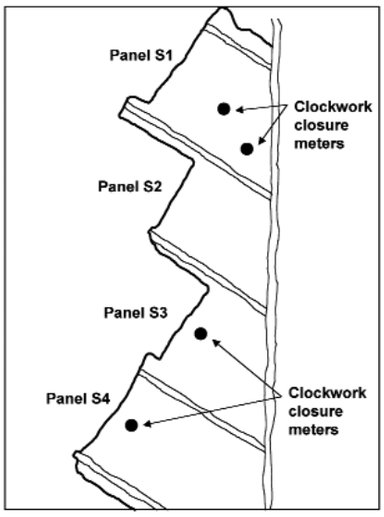

Figure 30—Installation positions of the closure meters in the various panels

three dominant sets of discontinuities in the hangingwall produced very poor hangingwall conditions and high rates of closure as shown in Figure 31.

The following sequence of four closure curves illustrate the rapid increase in closure experienced in one of the Merensky panels during November 2005. This data was initially used to motivate the stopping of blasting activity in the panel and subsequently to evacuate the panel after the accelerating rates of closure shown in Figure 35 were observed. A collapse in the face of the panel was reported after 30 November. The full extent of the fall is not known, however.

As a further example, monitoring was conducted on the UG2 reef horizon in an area where the middling between the UG2 and Merensky Reef is only approximately 18 m. The depth is approximately 1 200 m below surface. Significant ground control problems are experienced in the UG2 panels if these are mined below any remnants left on the Merensky Reef horizon. An example of a typical problem geometry is shown in Figure 36. The outline of the Merensky remnant is shown by the arrows. The UG2 panels (1N to 5N) were mining towards and below this Merensky remnant.

In overstoped areas far away from the remnant, the conditions in the UG2 panes are very good and the rate of closure is low (Figure 37).

Close to and below the remnants, the conditions in the panels, however, deteriorate rapidly and the rate of closure increases significantly. Figure 38 illustrates the onset of instability with joints opening up, small falls of ground and support units showing evidence of high rates of closure.

In these UG2 panels, the continuous closure measurements were found to be very useful to indicate proximity to the remnants as well as hazardous conditions. The sequence of closure curves below illustrates the rapid increase in closure for a panel below a Merensky remnant. Based on this data, the mine decided to abandon this particular panel. The rapid increase in closure was caused by the opening of two major joints (one on strike and one on dip), which intersected in the face area of the panel. This caused a major section of the hangingwall to become unstable.

Figure 31—Typical conditions in the Merensky stope described above. The high rate of closure caused the failure of the elongates in the foreground. Note the closure meter in the background

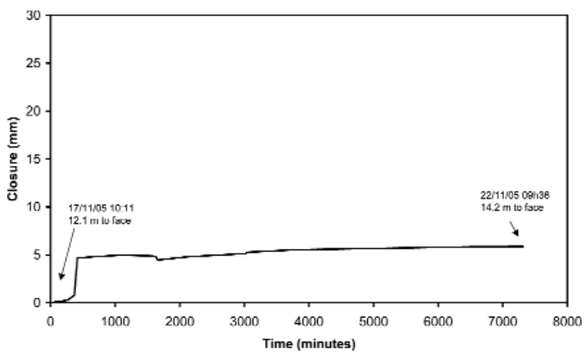

Figure 32—Closure in Panel S3 for the period 17/11/2005 to 22/11/2005. Note the rate of closure in the absence of blasting

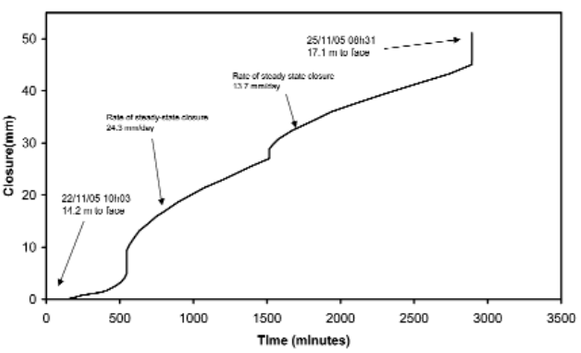

Figure 33—Closure in Panel S3 for the period 22/11/2005 to 25/11/2005. The rate of steady-state closure increased significantly after the blast on the 22nd

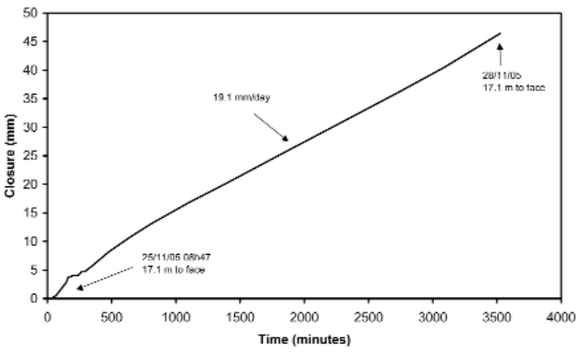

Figure 34—Closure in Panel S3 for the period 25/11/2005 to 28/11/2005. The high rate of steady-state closure persisted in the absence of any blasting

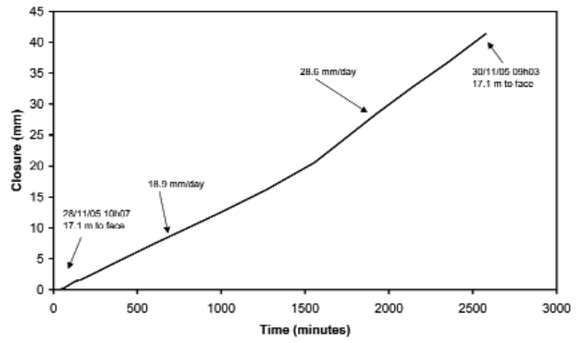

Figure 35—Closure in Panel S3 for the period 28/11/2005 to 30/11/2005. The rate of steady-state closure accelerated further in the absence of any blasting. Based on this information, the mine decided to evacuate and abandon these panels

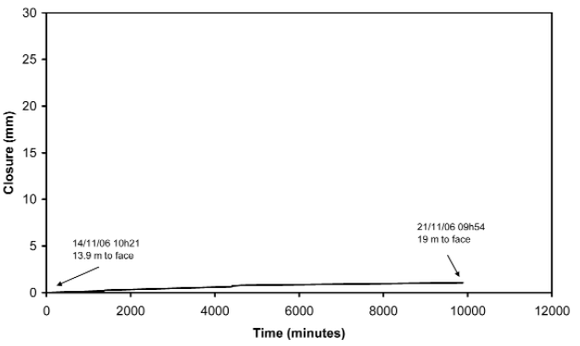

Figure 37—Low rate of closure in the UG2 panels in overstoped ground

Figure 38—Poor ground conditions and open joints in the UG2 panels when mining occurs in close proximity to the Merensky remnants

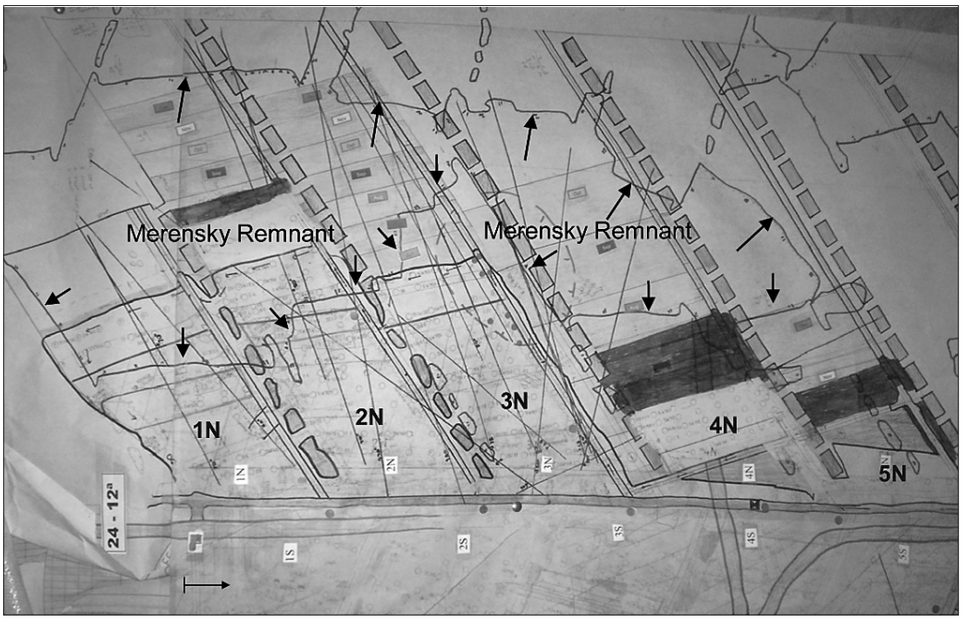

Figure 36—UG2 panels mining towards and below a Merensky remnant (the arrows show the outline of the remnant)

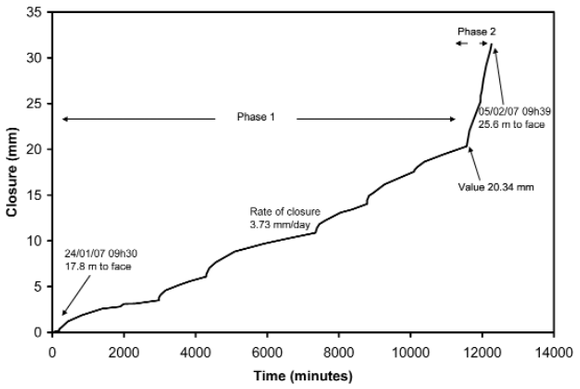

Figure 39—Continuous closure recorded for the period from 24/01/2007 to 05/02/2007. Note the rapid increase in closure towards the end of the graph

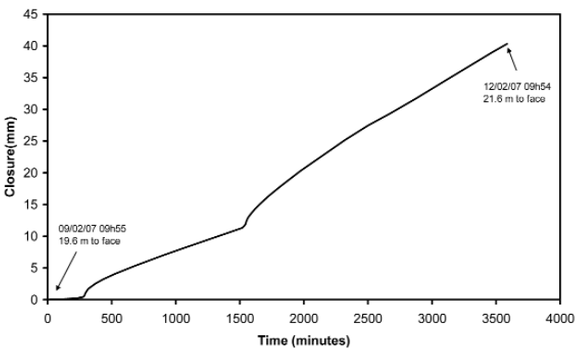

Figure 40—Continuous closure recorded for the period from 09/02/2007 to 12/02/2007

It should be noted that the closure measurements significantly enhance the hazard assessment and decision-making tools available to rock engineers. It would, however, be dangerous to attempt to use these closure measurements as a 'prediction' tool for all falls of ground as it was found that in some cases the warning period may be short (Figure 42), or the closure meter may be installed too far away from the collapse to provide any warning. Further work to investigate the precursors obtained from the data and the period of warning will have to be conducted.

Identification of areas prone to strain bursting

Preconditioning has been proven to be a very effective tool to combat face-bursting problems experienced in the some areas of the gold mining industry (e.g. Kullmann *et al*[57]). It has nevertheless always been difficult to decide which areas to

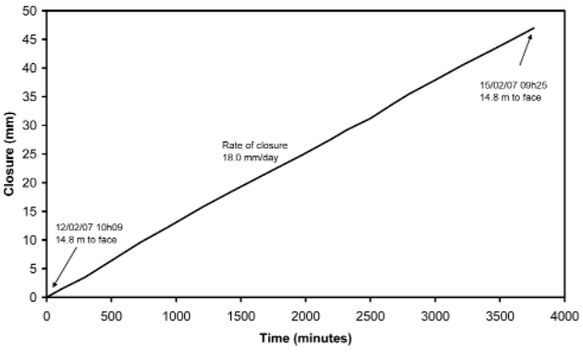

Figure 41—Continuous closure recorded for the period from 12/02/2007 to 15/02/2007. Note the very high rate of steady-state closure compared to that in Figure 15 before the failure. Based on this information, the mine decided to abandon this panel

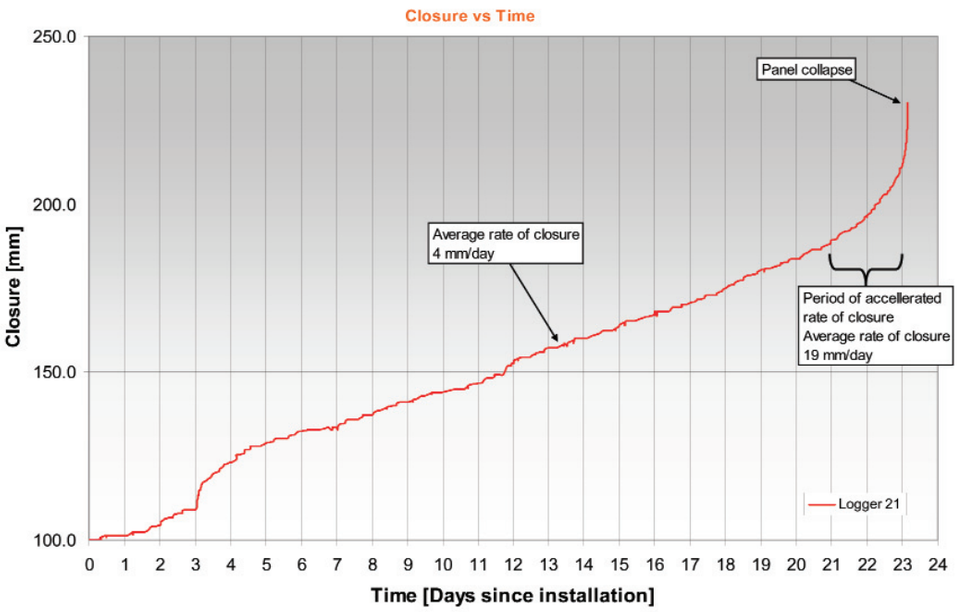

Figure 42—Closure recorded prior to a collapse in a UG2 panel. A two-day period of accelerated closure was observed prior to the collapse

precondition and unfortunately implementation of this technique seems to be mostly reactive after face-bursting accidents occurred. From the closure studies, it was found that in highly stressed areas with a high average $\Delta S_I/\Delta S_T$ ratio, face bursting is a common occurrence and these areas benefit hugely from the implementation of preconditioning. An example of the closure behaviour of such an area has already been shown in Figure 13a. The reader should also refer to the earlier comments in the paper about the use of the $\Delta S_I/\Delta S_T$ ratio. This ratio was found useful only in relation to identification of areas prone to face bursting events and will not give any indication of seismic risk in terms of events that originate on large geological structures.

In contrast, areas with a low average $\Delta S_I/\Delta S_T$ ratio (Figure 13b) seem to rarely encounter strain bursting problems. Closure measurements can and should therefore be used as an additional tool to decide on the implementation of preconditioning.

Although stopes with low average $\Delta S_I/\Delta S_T$ ratios do not appear to experience face-bursting problems, these low ratios invariable imply that the rock mass is very 'mobile' and unstable hangingwall conditions are typically encountered. Observations show that for areas with low average $\Delta S_I/\Delta S_T$ ratios, an improvement in hangingwall conditions can be achieved by increasing the mining rate (as the face area of the stope then has less time to unravel).

Closure measurements to monitor the effectiveness of preconditioning

A further problem encountered with preconditioning is to measure the effectiveness of the technique after implementation. The use of continuous closure data appears to be a very useful tool in this regard. Continuous closure data was collected by the authors when preconditioning was introduced in the 87–49 longwall at Mponeng Mine. Typical results are illustrated in Figure 43. Note that the steady-state closure rate increases significantly after the onset of preconditioning. This is further illustrated in Figure 44, which compares the rate of steady state closure as a function of distance from the face for panels with and without preconditioning. It is clear from this that the steady-state creep rate is significantly increased with preconditioning. This suggests that the size of the fracture zone ahead of the stope face is increased or the pre-existing fractures are mobilized, allowing the strain energy stored near the stope face to be reduced and decreasing the likelihood of face bursting.

Data for improved stope support design

Rate of closure (expressed as mm per metre advance or mm per day) is an important parameter for support design. Especially in the deep gold mines with seismic problems, the energy absorption capability of support units is an important design parameter. Rock engineers need to calculate at what distance from the face the energy absorption capability of the support units has been 'depleted' by the rate of closure. Unless the time-dependent component of closure is quantified, it is not clear what the effect of mining rate will be on the rate of closure. This should not be ignored. Unfortunately the use of the popular 'mm/m' unit for rate of closure inherently implies that there is no time-dependent closure component.

As mentioned above, for support design, it is important to quantify the amount of closure that will act on a support unit from installation until it is a certain distance behind the face. This is illustrated in Figure 45. In this particular example, the support unit is installed 3 m from the face on a specific day. After a period of time, the face has been advanced by 5 m, putting the support unit at distance of 8 m from the face. As the rate of closure contains a time-dependent component, which persists even if there is no

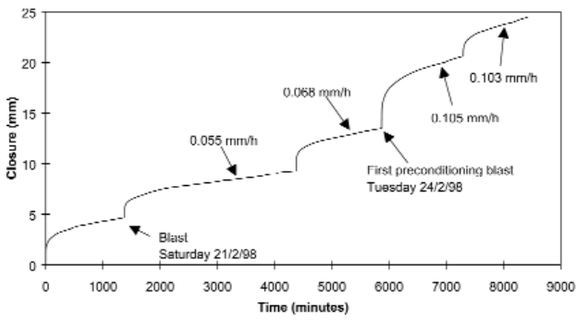

Figure 43—The effect of preconditioning on the time-dependent closure of a stope in the Ventersdorp Contact Reef. The instrument was 7.2 m from the face at the beginning of this data set and 10.5 m from the face after the last blast in the figure

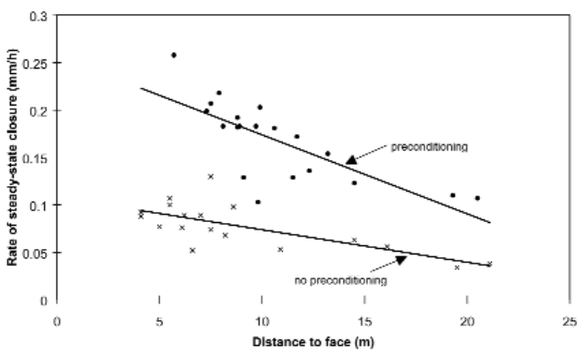

Figure 44—The effect of preconditioning on the rate of steady-state closure for panels in the Ventersdorp Contact Reef

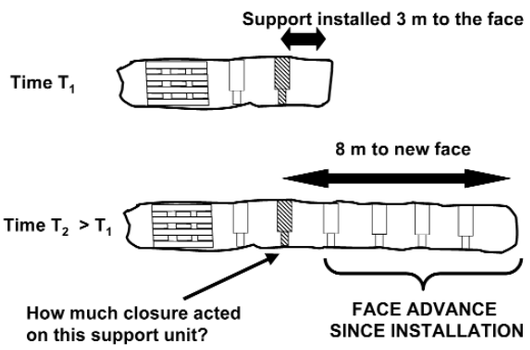

Figure 45—Example to illustrate the effect of mining rate on rate of closure

mining activity, the total closure acting on this support unit will be dependent on the mining rate and the total elapsed time.

The total daily closure, S^i_{daily}, acting on a support unit on a particular day i (where i = 1,2,3... to denote successive days) can be given by the Equation (see Figure 4):

$$S^i_{daily} = S^i_I + S^i_P + S^i_{SS} \quad [26]$$

If there is no blasting (or large seismic events), the instantaneous and primary closure components are zero and Equation [26] reduces to

$$S^i_{daily} = S^i_{SS} \quad [27]$$

For the example in Figure 45, the total closure can now be calculated for different mining rates. If blasting occurs every day (five days to advance 5 m) the total closure acting on the support unit is

$$S_{TOTAL} = \sum_{i=1}^{5} S^i_{daily} = \sum_{j=1}^{5} \left(S^j_I + S^j_P\right) + \sum_{i=1}^{5} S^i_{SS} \quad [28]$$

where j denotes each successive mining increment. The first term in Equation [28] denotes the sum of the instantaneous and primary closure following each blast (assumed to be independent of mining rate), while the second term is the sum of all the time-dependent closure. If, however, blasting occurs only every second day (10 days to advance 5 m), the total closure acting on the support unit will be

$$S_{TOTAL} = \sum_{i=1}^{10} S^i_{daily} = \sum_{j=1}^{5} \left(S^j_I + S^j_P\right) + \sum_{i=1}^{10} S^i_{SS} \quad [29]$$

When one compares Equations [28] and [29], it can be seen that the total closure acting on the support unit will be larger for the slower mining rate, even though the total face advance is 5 m in both cases. The difference in closure magnitude acting on the support unit for various mining rates will depend on the rate of steady-state closure. The larger the rate of steady-state closure, the bigger the effect of the mining rate. To quantify this effect, the following technique was developed from the underground observations.

The rate of steady-state closure appears to be constant in the short term but it gradually decreases when there is no blasting or seismic activity. This is illustrated in Figure 46. The measurements were obtained over a long weekend when there was no mining activity for several days. The steady-state closure is best approximated by a function of the form

$$S_{SS} = a\left(1 - e^{-bt)}\right) \quad [30]$$

where a and b are parameters and t is time. The steady-state closure for station No. 2 in Figure 46 after the seismic event was plotted in Figure 47 together with the model given in Equation [30]. The parameters used to obtain this fit were a = 3.85 mm and b = 0.015 h^{-1}. Note that these values are applicable only to this particular stope.

From Equation [30], the rate of steady-state closure is given by

$$\frac{dS_{SS}}{dt} = ce^{-bt} \quad [31]$$

where $c = ab$. From Equation [31], the rate of steady-state closure at t = 0 is given by c. For convenience, Equation [30] will be written as

$$S_{SS} = \frac{c}{b}\left(1 - e^{-bt)}\right) \quad [32]$$

Continuous closure measurements indicate that the rate of steady-state closure is also a function of measurement position in the panel. This is indicated in Figure 48 where the rate of steady-state closure appears to decrease as the

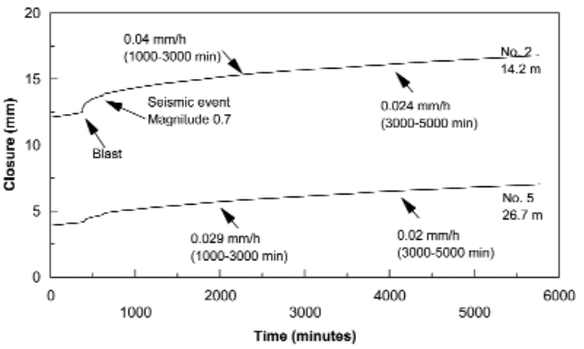

Figure 46—Closure measured in a VCR (hard lava) panel when there was no mining activity for a period of four days. The time periods in brackets indicate the intervals used to calculate the steady-state closure rates. Two closure instruments at different distances to the face were used to collect the data

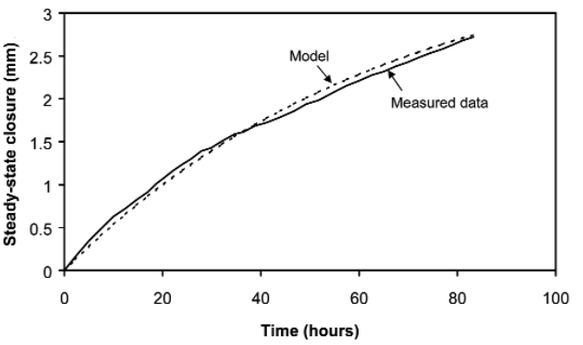

Figure 47—Measured and simulated values of steady-state closure for the VCR (hard lava) panel

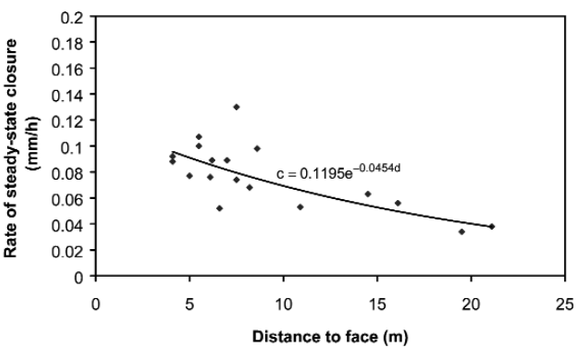

Figure 48—Effect of distance to face on the rate of steady-state closure. Although there is some scatter present in the data with a resulting poor fit to the given function, it was used as a useful approximation of the trend

distance to face increases. The parameter c in Equation [32] is therefore a function of the distance to face. As the rate of steady-state closure is also a function of the length of face advance on a particular day and the position in the panel along strike, there is some scatter present in the data as illustrated in Figure 48. From studies described in Malan[19], where three closure meters were installed at increasing distance to the face, it is, however, clear that after any particular blast, the rate of steady-state closure decreases into the back area. The parameter c will therefore be approximated by the following function

$$c = \alpha e^{-\beta d} \qquad [33]$$

where d is the distance to face. From the fit in Figure 48, calibrated values for α and β are 0.1195 mm/h and 0.0454 m^{-1}, respectively. Inserting Equation [33] in [32] gives

$$\Delta S_{SS} = \frac{\alpha e^{-\beta d}}{b}\left(1 - e^{-bt}\right) \qquad [34]$$

As the decrease in rate of steady-state closure illustrated in Figure 47 is repeated after every blast, Equation [34] should be further modified to allow for the incremental enlargement of the stope. If a closure meter is installed at a fixed position in the stope and a number of increments are mined, the total amount of steady-state closure (S_{SS}^{T}) measured at that position will be given by

$$S_{SS}^{T} = \sum_{k=1}^{n} \frac{\alpha e^{-\beta(k\Delta\ell + f)}}{b}\left[1 - e^{-b(\tau_k - \tau_{k-1})}\right] \qquad [35]$$

where n is the number of mining increments and τ_k is the time when the kth increment is mined. The distance to face is given by

$$d = k\Delta\ell + f \qquad [36]$$

where $\Delta\ell$ is the size of each mining increment and f is the original distance to face. Equation [35] was used to simulate the effect of different mining rates (for a total face advance of 20 m) on the steady-state closure at a measuring point 5 m behind the original face. The size of each mining increment was assumed to be 1 m. The calibrated values for α, β and b obtained from Figures 47 and 48 were used. The results are illustrated in Figure 49. It is assumed that the parameters α and β are not functions of the mining rate. The effect of different mining rates is clearly visible in Figure 49. It should be emphasized that the closure plotted in Figure 49 is only the steady-state closure and does not include the instantaneous or primary closure components. Equation [35] can, however, be used to estimate how a wide range of mining rates will affect the rate of closure.

From Figure 49, note that at a distance of 10 m from the face (for support originally installed 5 m from the face), the cumulative steady-state closure is 8.4 mm for continuous mining operations. This gives a steady-state closure rate of 1.7 mm/m. If there is only one blast a week, the steady-state closure at the same distance to face will be 25.5 mm. The corresponding rate of closure is 5.1 mm/m, which is an increase of 3.4 mm/m. Imagine then that the stope is mined using continuous operations (blasting every day). Previous closure measurements during this period (for a closure station installed 5 m from the face) might indicate that the rate of total stope closure for a face advance of 5 m is some value, say mm/m. If it is decided to decrease the mining rate to just one blast a week, the new rate of closure that can be expected is (× +3.4) mm/m. The current support design should then be tested against this new estimated rate to establish if any changes are required.

Conclusions

This paper presents an overview of work carried out over several years to investigate the continuous stope closure profiles recorded in tabular excavations and the use of this data as a hazard indicator. The study is a useful example of the value of 'fundamental' research as the study of a poorly understood phenomenon led to some practical tools being developed for the mining industry.

The closure measurements indicated a significant time-dependent closure component in spite of the brittle nature of the rock. Time-dependent rates as high as 1 mm/hour have been measured in extreme cases. The time-dependent closure components appears to be ubiquitous in the gold mines and intermediate depth platinum mines and is even observed in very brittle environments such as VCR stopes with a Ventersdorp lava hangingwall. Although the limitations of elastic modelling has been known for many decades, this latest study further emphasized that caution must be

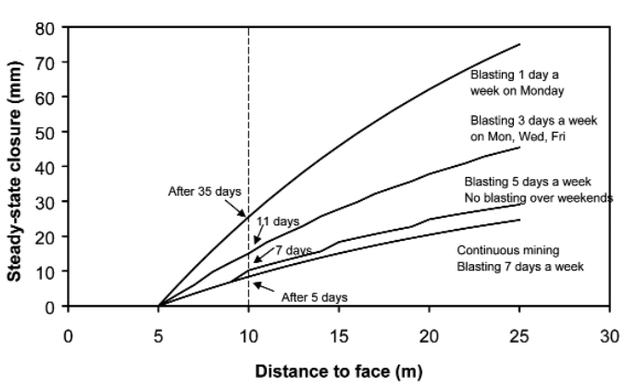

Figure 49—The effect of mining rate on the total amount of steady-state closure at a particular point in the stope

exercised when using elastic analysis to estimate stope closure as in some cases time-dependent closure will continue unabated for many days or weeks without any blasting or change in layout geometry.

Various approached to simulate the time-dependent closure have been investigated. Plane strain analytical solutions for the convergence of stope where the rock behaves as a Burgers viscoelastic material in distortion were derived. These models gave a reasonable fit to data recorded underground. Although viscoelastic theory therefore appears to be able to simulate time-dependent closure behaviour, there are subtle problems with the use of this theory as it cannot simulate the failure processes in the rock and care should be exercised when attempting to use these models.

To overcome these problems, continuum and discontinuum elasto-viscoplastic models have been developed. Discontinuum models have the advantage of being able to simulate the creep behaviour of prominent discontinuities. The development of these models has provided useful insights into rock mass deformation and has enabled the simulation of parameters such as rate of mining to be conducted for the first time.

A number of practical applications for the mining industry were developed from this study. Among these is the delineation of geotechnical areas using closure data, use of the data as a hazard indicator and to give warning of large collapses in the platinum mines, identification of areas in need of preconditioning in the gold mines, measurement of the effectiveness of preconditioning, and improved data for support design to include the effect of mining rate.

A number of issues still need to be researched further, such as the type of precursory information obtained from closure data prior to large collapses. It appears that different warning periods are currently obtained from the data and the reasons for this are not well understood. In platinum mines, the contribution of time-dependent pillar crushing to the stope closure needs to be researched. It is hypothesized that the time-dependent closure components will be less in areas with oversize pillars experiencing seismicity. This may lead to routine monitoring and modelling strategies that can be used to identify areas in platinum mines that will be prone to pillar bursting. Further work using time-dependent seam failure models in 3D boundary element models also needs to be conducted to investigate the appropriateness of using this to simulate time-dependent stope behaviour on a large scale. Generalizing the concept of ERR to an inelastic time-dependent ERR can lead to an improved assessment of the stability of mining excavations.

Acknowledgements

The authors wish to acknowledge the financial assistance and support received from the Safety in Mines Research Advisory Committee (SIMRAC), who sponsored most of this work.

References

1. Malan, D.F. A viscoelastic approach to the modelling of the transient closure behaviour of tabular excavations after blasting. *J. S. Afr. Inst. Min. Metall.* vol. 95, 1995, pp. 211–220.

2. Napier, J.A.L., Hildyard, M.W., Kuijpers, J.S., Daehnke, A., Sellers, E.J., Malan, D.F., Siebrits, E., Ozbay M.U., Dede, T., and Turner, P.A. Develop a quantitative understanding of rockmass behaviour near excavations in deep mines. Final SIMRAC project report (GAP029). 1995.

3. Napier, J.A.L., Malan, D.F., Sellers, E.J., Daehnke, A., Hildyard, M.W., Dede, T., and Shou, K-J. Deep gold mine fracture zone behaviour, Final SIMRAC project report (GAP332), 1999.

4. Napier, J.A.L., Dresher, K., Hildyard, M.W., Kataka, M.O., Malan, D.F., and Sellers, E.J. Experimental investigation of fundamental processes in mining induced fracturing and rock instability. Final SIMRAC project report (GAP601b), 2002.

5. Malan, D.F., Kononov, V.A., Coetzer, S.J., Janse van Rensburg, A.L., and Spottiswoode, B.S. The feasibility of a mine-wide continuous closure monitoring system for gold mines, Final Project Report, SIMRAC GAP705, Sept, 2000.

6. Malan, D.F., Grave, M., Napier, J.A.L., Piper, P.S., and Lawrence, L.E. Experimental validation of a mine-wide continuous closure monitoring system as a decision making tool for gold mines: Final Project Report, SIMRAC GAP852, March 2003

7. Roberts, D.P., Malan, D.F., Janse van Rensburg, A.L., Grodner, M.W., and Handley R. Closure profiles of the UG2 and Merensky Reef Horizons at various depths, using different pillar types , in the Bushveld Complex. Final project report, SIMRAC SIM 040207, March 2006.

8. Malan, D.F., Janse van Rensburg, A.L., and Roberts, D.P., Closure monitoring as a design and risk assessment tool in platinum mines. *Proc. SARES 2005 3rd Southern African Rock Engineering Symposium*, The South African Institute of Mining and Metallurgy, Symposium Series S41, 2005. pp. 231–243.

9. Ryder, J.A. and Officer, N.C. An elastic analysis of strata movement observed in the vicinity of inclined excavations. *J. S. Afr. Inst. Min. Metall.*, vol. 64, no. 6, 1964. pp. 219–244.

10. Salamon, M.D.G. Elastic analysis of displacements and stresses induced by the mining of reef deposits. *J. S. Afr. Inst. Min. Metall.*, vol. 64, 1964, pp. 128–149.

11. Cook, N.G.W., Hoek, E., Pretorius, J.P.G., Ortlepp, W.D., and Salamon, M.D.G. Rock mechanics applied to the study of rockbursts. *J. S. Afr. Inst. Min. Metall.*, vol. 66. 1966. pp. 435–528.

12. Napier, J.A.L. and Stephansen, S.J. Analysis of Deep-level Mine Design Problems Using the MINSIM-D Boundary Element Program, *APCOM 87. Proceedings of the Twentieth International Symposium on the Applications of Computers and Mathematics in the Mineral Industries.* Volume 1: Mining. Johannesburg, SAIMM, 1987. pp. 3–19.

13. Ryder. J.A. and Jager, T. *A textbook on rock mechanics for tabular hard rock mines*. SIMRAC, 2002.

14. Salamon, M.D.G. Energy considerations in rock mechanics: Fundamental results. *J. S. Afr. Inst. Min. Metall.*, vol. 84, no. 8, 1984. pp. 223–246.

15. Napier, J.A.L. Energy changes in a rockmass containing multiple discontinuities. *J. S. Afr. Inst. Min. Metall.*, vol. 91, no. 5, 1991. pp. 145–157.

16. ISRM terminology booklet, 1975

17. Altson, B.T. Remarks on sand-filling. *Pap. Ass. Min. Mngrs. S.Afr.*, 1931–1936: 1933. pp. 429–432.

18. Mickel, R.E. Pressure bursts. *Pap. Ass. Min. Mngrs. S.Afr.*, 1931–1936: 1935. pp. 394–428.

19. Malan, D.F. An investigation into the identification and modelling of time-dependent behaviour of deep level excavations in hard rock. PhD Thesis, University of the Witwatersrand, Johannesburg, 1998.

20. HILL, F.G. An experiment in support at depth at the East Rand proprietary Mines, Limited. *Pap. Ass. Min. Mngrs. S.Afr.*, 1942–1945: 1942. pp. 413–420.

21. BARCA, M. and VON WILLICH, G.P.R. Strata movement measurements at Harmony Gold Mine. *Pap. Ass. Min. Mngrs. S.Afr.*, 1958–1959: 1958. pp. 447–464.

22. WIGGILL, R.B. The effects of different support methods on strata behaviour around stoping excavations. Symposium on Rock Mechanics and Strata Control in Mines: *J. S. Afr. Inst. Min. Metall.* 1965. pp. 1–35.

23. LEEMAN, E.R. Some measurements of closure and ride in a stope of the East Rand Proprietary Mines. *Pap. Ass. Min. Mngrs. S.Afr.*, 1958–1959: 1958. pp. 385–404.

24. ORTLEPP, W.D. and NICOLL, A. The elastic analysis of observed strata movement by means of an electrical analogue. *J. S. Afr. Inst. Min. Metall.* vol. 65, no. 4, 1964. pp. 214–235.

25. HODGSON, K. The behaviour of the failed zone ahead of a face, as indicated by continuous seismic and convergence measurements, Chamber of Mines Research Report 31/61, Transvaal and Orange Free State Chamber of Mines Research Organisation, 1967.

26. MCGARR, A. Stable deformation near deep-level tabular excavations. *J. Geophys. Res.*, vol. 76, no. 29, 1971. pp. 7088–7106.

27. WALSCH, J.B., LEYDE, E.E., WHITE, A.J.A., and CARRAGHER, B.L. Stope closure studies at West Driefontein gold mine. *Int. J. Rock Mech. Min. Sci & Geomech. Abstr.*, vol. 14. 1977. pp. 277–281.

28. KING, R.G., JAGER, A.J., ROBERTS, M.K.C., and TURNER, P.A. Rock mechanics aspects of stoping without back-area support. COMRO Research Report, no. 17/89, 1989.

29. GÜRTUNCA, R.G. Results of a classified tailings monitoring programme at Vaal Reefs. COMRO Internal Report, no. 614, 1989.

30. GÜRTUNCA, R.G., JAGER, A.J., ADAMS, D.J., and GONLAG, M. The *in situ* behaviour of backfill materials and the surrounding rockmass in South African gold mines. Hassani, F. (ed.) *Proc. 4th Int. Symp. of Mining with Backfill.*, Balkema, Rotterdam, 1989. pp. 187–197.

31. GÜRTUNCA, R.G. and ADAMS, D.J. Determination of the *in situ* modulus of the rockmass by the use of backfill measurements. *J. S. Afr. Inst. Min. Metall.* vol. 91, no. 3, 1991. pp. 81–88.

32. PIPER, P. and GÜRTUNCA, R.G. Measuring convergence and ride. *SANGORM News*, Johannesburg, February 1987.

33. PIPER, P., GÜRTUNCA, R.G., and MARITZ, R.J. Instrumentation to quantify the *in situ* stress-strain behaviour of mine backfill. *MINEFILL 93*, SAIMM, Johannesburg, 1993. pp. 109–120.

34. GÜLER, G. Analysis of the rock mass behaviour as associated with Ventersdorp Contact Reef stopes, South Africa. MSc dissertation: University of the Witwatersrand: Johannesburg, 1998.

35. MALAN, D.F. and NAPIER, J.A.L. The effect of geotechnical conditions on the time-dependent behaviour of hard rock in deep mines. Amadei, B., Kranz, R.L., Scott, G.A. and Smeallie, P.H. (eds.) *37th U.S. Rock Mechanics Symposium,* Vail Rocks '99, Balkema, 1999. pp. 903–910.

36. MALAN, D.F. Time-dependent behaviour of deep level tabular excavations in hard rock. *Rock Mech. Rock Eng.*, vol. 32, no. 2, 1999. pp. 123–155.

37. MALAN, D.F., JANSE VAN RENSBURG, A.L., and ROBERTS, D.P. Closure monitoring as a design and risk assessment tool in platinum mines. *SARES 2005 3rd Southern African Rock Engineering Symposium*, The South African Institute of Mining and Metallurgy, Symposium Series S41, 2005. pp. 231–243.

38. FLÜGGE, W. *Viscoelasticity*. 2nd edition, New York, Springer-Verlag, 1975.

39. LAMA, R.D. and VUTUKURI, V.S. *Handbook on mechanical properties of rocks—Testing techniques and results*. Volume III. Trans Tech Publications, Germany, 1978. pp. 209–320.

40. ROBERTSON, E.C., Viscoelasticity of Rocks. Judd, W.R. (ed.) *State of stress in the Earth's crust. Proc. Int. Conf.*, Santa Monica, California, 1964. pp. 181–233.

41. PAN, Y.W. and DONG, J.J. Time-dependent tunnel convergence - I. Formulation of the model. *Int. J. Rock Mech. Min. Sci.*, vol. 28, 1991. pp. 469–475.

42. GIODA, G. On the non-linear 'squeezing' effects around circular tunnels. *Int. J. Num. Anal. Meth. Geomech.*, vol. 6, 1982. pp. 21–46.

43. GIODA, G. and CIVIDINI, A. Numerical methods for the analysis of tunnel performance in squeezing rocks. *Rock Mech. Rock Engng.*, vol. 29, 1996. pp. 171–193.

44. AKAGI, T., ICHIKAWA, Y., KURODA, H., and KAWAMOTO, T. A non-linear rheological analysis of deeply located tunnels. *Int. J. Num. Anal. Meth. Geomech.*, vol. 8, 1984. pp. 457–471.

45. SONG, D. Non-linear viscoplastic creep of rock surrounding an underground excavation. *Int. J. Rock Mech. Min. Sci. & Geomech. Abstr.*, vol. 30, 1993. pp. 653–658.

46. LEE, C., LEE, Y., and CHO, T. Numerical simulation for the underground excavation-support sequence in the visco-plastic jointed rock mass. Fujii, T. (ed.) *Proc. 8th Int. Cong. Rock Mech., ISRM*, Balkema, Rotterdam, 1995. pp. 619–621.

47. PERZYNA, P. Fundamental problems in viscoplasticity. *Adv. Appl. Mech.*, vol. 9, 1966. pp. 243–377.

48. DESAI, C.S. and ZHANG, D. Viscoplastic model for geologic materials with generalised flow rule. *Int. J. Num. Anal. Meth. Geomech.*, vol. 11, 1987. pp. 603–620.

49. SEPEHR, K. and STIMPSON, B. Potash mining and seismicity: A time-dependent finite element model. *Int. J. Rock Mech. Min. Sci & Geomech. Abstr.*, vol. 25, 1988. pp. 383–392.

50. FAKHIMI, A.A. and FAIRHURST, C. A model for the time-dependent behavior of rock. *Int. J. Rock Mech. Min. Sci.*, vol. 31, 1994. pp. 117–126.

51. MALAN, D.F. Time-dependent behaviour of deep level tabular excavations in hard rock. *Rock Mech. Rock Engng.*, vol. 32, 1999. pp. 123–155.

52. MALAN, D.F. Implementation of a viscoplastic model in FLAC to investigate rate of mining problems. Detournay, C and Hart, R. (eds.) *FLAC and Numerical Modelling in Geomechanics, Proc of the Int. FLAC Symp on Num. Modelling in Geomech.*, Minnesota, Balkema, 1999. pp. 497–504.

53. NAWROCKI, P.A. One-dimensional semi-analytical solution for time-dependent behaviour of a seam. *Int. J. Num. Anal. Meth. Geomech.*, vol. 19, 1995. pp. 59–74.

54. NAPIER, J.A.L. and MALAN, D.F. A viscoplastic discontinuum model of time-dependent fracture and seismicity effects in brittle rock. *Int. J. Rock Mech. Min. Sci. & Geomech. Abstr*, vol. 34, 1997. pp. 1075–1089.

55. MALAN, D.F., NAPIER, J.A.L., and GRAVE, M. Experiments on stope closure as a diagnostic measure of rock behaviour. Handley, M. and Stacey, D. (eds.) *International Society for Rock Mechanics, 10th Congress*, Sandton, SAIMM Symposium series S33, 2003. pp. 795–801.

56. MALAN, D.F. Rock mass monitoring as a hazard assessment tool in deep Merensky and UG2 stopes. *Proc. 11th ISRM Congress*, Lisbon, 2007.

57. KULLMANN, D.H., STEWART, R.D., and GRODNER, M. A pillar preconditioning experiment on a deep-level South African gold mine, M. Aubertin, F. Hassani and H. Mitri (eds.) *Proc. 2nd North Am. Rock Mech. Symp: NARMS '96,* Montreal, 1996. pp. 375–380. ◆